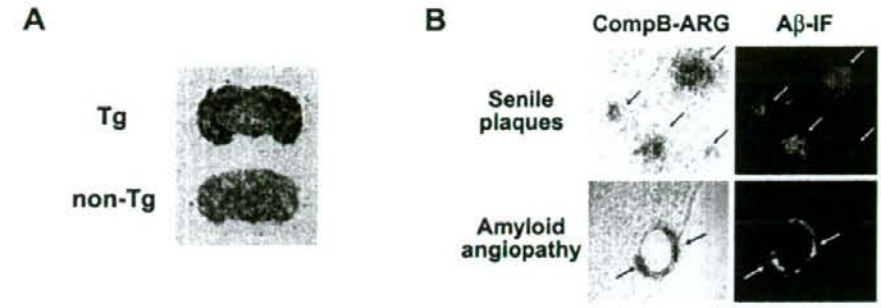

Fig. (4). Amyloid imaging of compB in an Alzheimer's disease mouse model.
A. Autoradiogram of the brain tissue section from an Alzheimer's disease model mouse (Tg) or a control mouse (non-Tg) with an intravenous injection of radio-labeled compB. The brains were obtained 5 h after injection.
B. Microautoradiogram (CompB-ARG) and Aβ immunohistochemistry (Aβ-IF) of an identical section from the same brain tissue of an Alzheimer's disease model mouse shown in A.

CompB is lipophilic and has an excellent permeability into the brain involving no active efflux system [48,51]. However, aside from its low metabolic stability in mouse liver microsome, it has high inhibition activities against several common P450 isozymes, which potentially causes a drug-drug interaction problem [51]. Therefore, the safety properties and pharmacokinetic parameters of this compound must be improved before its clinical application can be considered.

FURTHER IMPROVEMENT

The findings of amyloidophilic compounds described here indicate that the compounds are useful not only for prion amyloid imaging but also for therapy. Especially, the findings related to an orally available amyloidophilic chemical, compB, are encouraging. However, disease progression is not halted even when treatment commences immediately after the infection and continues to the terminal stage of disease.

One reason for this limited effectiveness might be connected with the prion strain-dependent efficacies of the amyloidophilic compounds. Prion strains definitely influence the outcomes of treatment with the compounds. The compounds are most effective against RML prion but less effective against 22L prion and Fukuoka-1 prion either *in vitro* or *in vivo*. They are never effective or only marginally effective against the 263K prion. Interestingly, the PrPsc glycoform patterns observed in the compB-treated mice are predominantly diglycosylated and similar to that of 263K prion, although a monoglycoform predominant pattern is observed in non-treated mice [48]. Such pattern characteristics suggest that limitations of compB efficacy might result from the appearance of compB-resistant diglycoform predominant prions.

Another possible reason for the limited effectiveness might be related to pharmacokinetic properties of the compounds: CompB and BF-168, but not BSB are washed rapidly out from either the brain or the blood. Contrasting BF-168 to BSB shows that BSB prolongs the incubation periods of infected animals significantly longer than BF-168, although BSB requires less frequent intravenous injections and later application in the disease stage than BF-168. Therefore, not only permeability but also retention of chemicals in the brain is apparently important for better efficacies *in vivo*. In addition, metabolic stability of chemicals is definitely influential on their effectiveness.

Recently, Sigurdson and his colleagues observed prion strain-dependent fluorescence spectral shifts of luminescent conjugated polymers composed of thiophene derivatives when bound to PrPsc, demonstrating prion strain-dependent conformational properties of PrPsc [52], because the fluorescence spectra reflects distributions of the dihedral rotational angles among the monomeric units of the polymers [53,54]. In addition, the correlation between the dihedral rotational angle and the spectra gives insight into the binding mode of Congo red to amyloid [55,56]. On the other hand, rotational freedom between the aromatic rings of Congo red derivatives is important for their antiprion activities [31]. Restriction of the rotational freedom at the center of the compounds reduces the antiprion activities. In fact, compB comprises two aromatic ring parts connected by hydrazone in which free rotation is obtained at the imino nitrogen (-NH-). Similar compounds, 8-hydroxy-8-quinolinylhydrazone-2-quinolinecarboxaldehyde (QCQH in the reference) and 2-quinolinylhydrazone-2-pyridinecarboxaldehyde (PCQH in the reference) which were tested as quinoline derivatives, also have excellent antiprion activities [57]. These findings indicate that elucidation of the interaction between chemicals and PrPsc at the atomic level is necessary to facilitate further improvement of therapeutic candidates.

CONCLUSION

Amyloidophilic compounds are useful as both prion amyloid imaging probes and therapeutic candidates for prion diseases. The mechanism of the prion strain-dependent effectiveness of these compounds must be elucidated and managed. Nevertheless, the identification of compB, an orally available amyloidophilic chemical, encourages the pursuit of chemotherapy for prion diseases. Drug search and development for prion diseases reportedly does not interest

Table 1. *In Vitro* Activities of Phenylhydrazine Derivatives

Compound	Chemical structure	Molecular weight	Octanol-water distribution coefficient ($LogD_{6.5}$)	Inhibition of PrPsc formation (EC_{50}, nM)	Inhibition of Aβ amyloid formation (EC_{50}, μM)	Inhibition of Aβ amyloid-heparin binding (EC_{50}, μM)
CompB	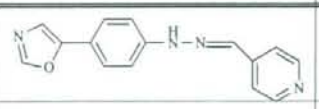	264	4.1	0.06	2.9	1.1
CompD1	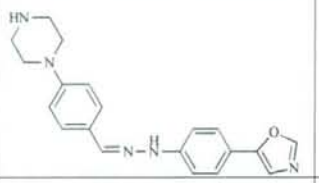	347	2.2	100	8.1	0.9
CompD2	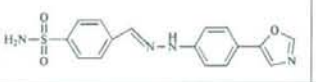	342	3.6	10	2.6	0.4
CompD3	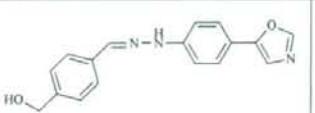	293	3.2	1	1.5	0.9
CompD4	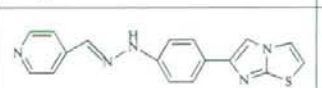	319	Not determined	1	1.1	0.4
CompD5	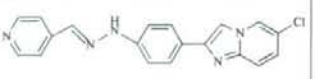	347	4.7	1	0.2	0.3
CompD6	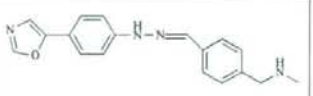	306	2.4	10	3.1	1.2

pharmaceutical companies because of the limited number of patients. However, a therapeutic linkage between prion diseases and other amyloidotic conditions such as AD, demonstrated by compB, might accelerate the development of therapeutic drugs for prion diseases.

ACKNOWLEDGMENTS

The studies described herein were supported by grants from the Ministry of Health, Labour and Welfare and from the Ministry of Education, Culture, Sports, Science and Technology, Japan.

ABBREVIATIONS

AD = Alzheimer's disease

BBB = Blood brain barrier

BF-168 = 2-(5-(2-fluoroethoxy)benzo[d]oxazol-2-yl)vinyl)-*N*-methylbenzenamine

BSB = (*trans, trans*),-1-bromo- 2,5-bis-(3-hydroxycarbonyl-4-hydroxy)styrylbenzene

BTA-1 = 2-[49-(methylamino)phenyl] benzothiazole

CJD = Creuzfeldt-Jakob disease

compB = 1-(4-(oxazol-5-yl)phenyl)-2-((pyridin-4-yl)methylene)hydrazine

EC_{50} = dose producing 50% maximal effect

GAG = Glycosaminoglycan

GSS = Gerstmann-Sträussler-Scheinker syndrome

PET = Positron emission tomography

PPS = Pentosan polysulfate

PrPc = Normal isoform of prion protein

PrPsc = Abnormal isoform of prion protein

REFERENCES

[1] Prusiner, S.B. *Science*, **1991**, *252*, 1515.
[2] Caughey, B.W.; Dong, A.; Bhat, K.S.; Ernst, D.; Hayes, S.F.; Caughey, W.S. *Biochemistry*, **1991**, *30*, 7672.
[3] Prusiner, S.B.; McKinley, M.P.; Bowman, K.A.; Bolton, D.C.; Bendheim, P.E.; Groth, D.F.; Glenner, G.G. *Cell*, **1983**, *35*, 349.
[4] Cohen, F.E.; Pan, K.M.; Huang, Z.; Baldwin, M.; Fletterick, R.J.; Prusiner, S.B. *Science*, **1994**, *264*, 530.
[5] Lansbury, P.T. *Science*, **1994**, *265*, 1510.
[6] Saborio, G.P.; Permanne, B.; Soto, C. *Nature*, **2001**, *411*, 810.
[7] Carrell, R.W.; Lomas, D.A. *Lancet*, **1997**, *350*, 134.
[8] Fred, P.; Anisimov, S.V.; Popovic, N. *Brain Res. Reviews* **2007**, *53*, 135.
[9] Divry, P. *J. Belge Neurol. Psychiatr.*, **1927**, *27*, 643.
[10] Kelényi, G. *Acta Neuropathol.*, **1967**, *7*, 336.
[11] Will, R.G.; Ironside, J.W.; Zeidler, M.; Cousens, S.N.; Estibeiro, K.; Alperovitch, A.; Poser, S.; Pocchiari, M.; Hofman, A.; Smith, P.G. *Lancet*, **1996**, *347*, 921.
[12] Brown, P.; Brandel, J.P.; Preece, M.; Sato, T. *Neurology*, **2006**, *67*, 389.
[13] Caughey, B.; Raymond, G.J. *J. Virol.*, **1993**, *67*, 643.
[14] Caughey, B.; Brown, K.; Raymond, G.J.; Katzenstein, G.E.; Thresher, W. *J. Virol.*, **1994**, *68*, 2135.
[15] Ingrosso, L.; Ladogana, A.; Pocchiari, M. *J. Virol.*, **1995**, *69*, 506.
[16] Cashman, N.R.; Caughey, B. *Nat. Rev. Drug Discov.*, **2004**, *3*, 874.
[17] Trevitt, C.R.; Collinge, J. *Brain*, **2006**, *129*, 2241.
[18] Stahl, N.; Borchelt, D.R.; Hsiao, K.; Prusiner, S.B. *Cell*, **1998**, *51*, 229.
[19] Snow, A.D.; Wight, T.N.; Nochlin, D.; Koike, Y.; Kimata, K.; Dearmond, S.J.; Prusiner, S. *Lab. Invest.*, **1990**, *63*, 601.
[20] Diringer, H.; Ehlers, B. *J. Gen. Virol.*, **1991**, *72*, 457.
[21] Farquhar, C.; Dickinson, A.; Bruce, M. *Lancet*, **1999**, *353*, 117.
[22] Mabbott, N.A.; MacPherson, G.G. *Nat. Rev. Microbiol.*, **2006**, *4*, 201.
[23] Dealler, S. *Lancet*, **1998**, *351*, 600.
[24] Doh-ura, K.; Kuge, T.; Uomoto, M.; Nishizawa, K.; Kawasaki, Y.; Iha, M *Antimicrob. Agents Chemother.*, **2007**, *51*, 2274.
[25] Irhimeh, M.R.; Fitton, J.H.; Lowenthal, R.M.; Kongtawelert, P. *Methods Find. Exp. Clin. Pharmacol.*, **2005**, *27*, 705.
[26] Jong, A.; Huang, S.H. *Curr. Drug Targets Infect. Disord.*, **2005**, *5*, 65.
[27] Doh-ura, K.; Ishikawa, K.; Murakami-Kubo, I.; Sasaki, K.; Mohri, S.; Race, R.; Iwaki, T. *J. Virol.*, **2004**, *78*, 4999.
[28] Rainov, N.G.; Tsuboi, Y.; Krolak-Salmon, P.; Vighetto, A.; Doh-Ura, K. *Expert Opin. Biol. Ther.*, **2007**, *7*, 713.
[29] Parry, A.; Baker, I.; Stacey, R.; Wimalaratna, S. *J. Neurol. Neurosurg. Psychiatry*, **2007**, *78*, 733.
[30] Bone, I.; Belton, L.; Walker, A.S.; Darbyshire, *J. Eur. J. Neurol.*, **2008**, *15*, 458.
[31] Demaimay, R.; Harper, J.; Gordon, H.; Weaver, D.; Chesebro, B.; Caughey, B. *J. Neurochem.*, **1998**, *71*, 2534.
[32] Okamura, N.; Suemoto, T.; Shimadzu, H.; Suzuki, M.; Shiomitsu, T.; Akatsu, H.; Yamamoto, T.; Staufenbiel, M.; Yanai, K.; Arai, H.; Sasaki, H.; Kudo, Y.; Sawada, T. *J. Neurosci.*, **2004**, *24*, 2535.
[33] Okamura, N.; Suemoto, T.; Furumoto, S.; Suzuki, M.; Shimadzu, H.; Akatsu, H.; Yamamoto, T.; Fujiwara, H.; Nemoto, M.; Maruyama, M.; Arai, H.; Yanai, K.; Sawada, T.; Kudo, Y. *J. Neurosci.*, **2005**, *25*, 10857.
[34] Cai, L.; Innis, R.B.; Pike, V.W. *Curr. Med. Chem.*, **2007**, *14*, 19.
[35] Furumoto, S.; Okamura, N.; Iwata, T.; Yanai, K.; Arai, H.; Kudo,Y. *Curr. Topics Med. Chem.*, **2007**, *7*, 1773.
[36] Bresjanac, M.; Smid, L.M.; Vovko, T.D.; Petric, A.; Barrio, J.R.; Popovic, M. *J. Neurosci.*, **2003**, *23*, 8029.
[37] Sadowski, M.; Pankiewicz, J.; Scholtzova, H.; Tsai, J.; Li, Y.; Carp, R.I.; Meeker, H.C.; Gambetti, P.; Debnath, M.; Mathis, C.A.; Shao, L.; Gan, W.B.; Klunk, W.E.; Wisniewski, T. *J. Neuropathol. Exp. Neuro.*, **2004**, *63*, 775.
[38] Smid, L.M.; Vovko, T.D.; Popovic, M.; Petric, A.; Kepe, V.; Barrio, J.R.; Vidmar, G.; Bresjanac. M. *Brain Pathol.*, **2006**, *16*, 124.
[39] Mathis, C.A.; Bacskai, B.J.; Kajdasz, S.T.; McLellan, M.E.; Frosch, M.P.; Hyman, B.T.; Holt, D.P.; Wang, Y.; Huang, G.F.; Debnath, M.L.; Klunk, W.E. *Bioorg. Med. Chem. Lett.*, **2002**, *12*, 295.
[40] Skovronsky, D.M.; Zhang, B.; Kung, M.P.; Kung, H.F.; Trojanowski, J.Q.; Lee, V.M. *Proc. Natl. Acad. Sci. USA*, **2000**, *97*, 7609.
[41] Ishikawa, K.; Doh-ura, K.; Kudo, Y.; Nishida, N.; Murakami-Kubo, I.; Ando, Y.; Sawada, T.; Iwaki, T. *J. Gen. Virol.*, **2004**, *85*, 1785.
[42] Ando, Y.; Haraoka, K.; Terazaki, H.; Tanoue, Y.; Ishikawa, K.; Katsuragi, S.; Nakamura, M.; Sun, X.; Nakagawa, K.; Sasamoto, K.; Takesako, K.; Ishizaki, T.; Sasaki, Y.; Doh-ura, K. *Lab. Invest.*, **2003**, *83*, 1751.
[43] Race, R. E.; Caughey, B.; Graham, K.; Ernst, D.; Chesebro, B. *J. Virol.*, **1988**, *62*, 2845.
[44] Nishida, N.; Harris, D.A.; Vilette, D.; Laude, H.; Frobert, Y.; Grassi, J.; Casanova, D.; Milhavet, O.; Lehmann, S. *J. Virol.*, **2000**, *74*, 320.
[45] Fischer, M.; Rulicke, T.; Raeber, A.; Sailer, A.; Moser, M.; Oesch, B.; Brandner, S.; Aguzzi, A.; Weissmann, C. *EMBO J.*, **1996**, *15*, 1255.
[46] Race, R.E.; Priola, S.A.; Bessen, R.A.; Ernst, D.; Dockter, J.; Rall, G.F.; Mucke, L.; Chesebro, B.; Oldstone, M.B. *Neuron*, **1995**, *15*, 1183.
[47] Ishikawa, K.; Kudo, Y.; Nishida, N.; Suemoto, T.; Sawada, T.; Iwaki, T.; Doh-ura, K. *J. Neurochem.*, **2006**, *99*, 19.
[48] Kawasaki, Y.; Kawagoe, K.; Chen, C.J.; Teruya, K.; Sakasegawa, Y.; Doh-ura, K. *J. Virol.*, **2007**, *81*, 12889.
[49] Kawagoe, K.; Motoki, K.; Odagiri, T.; Suzuki, N.; Chen, C.J.; Mimura, T. *PCT Int. Appl.*, **2004**, pp236.
[50] Hsiao, K.; Chapman, P.; Nilsen, S.; Eckman, C.; Harigaya, Y.; Younkin, S.; Yang, F.; Cole, G. *Science*, **1996**, *274*, 99.
[51] Suzuki, N.; Chen, C.J.; Kawagoe, K.; Motoki, K.; Odagiri, T.; Mimura, T. unpublished data.
[52] Sigurdson, C.J.; Nilsson, K.P.R.; Hornemann, S.; Manco, G.; Polymenidou, M.; Schwarz, P.; Leclerc, M.; Hammarström, P.; Wüthrich, K.; Aguzzi, A. *Nature Method*, **2007**, *4*, 1023.
[53] Nilsson, K.P.R.; Herland, A.; Hammarstrom, P.; Inganaas, O. *Biochemistry*, **2005**, *44*, 3718.
[54] Nilsson, K.P.; Hammarstrom, P.; Ahlgren, F.; Herland, A.; Schnell, E.A.; Lindgren, M.; Westermark, G.T.; Inganas, O. *Chem. Bio. Chem.*, **2006**, *7*, 1096.
[55] Elhaddaoui, A.; Merlin, J.C.; Delacourte, A.; Turrell, S. *J. Mol. Struct.*, **1992**, *267*, 113.
[56] Miura, T.; Yamamiya, C.; Sasaki M.; Suzuki K.; Takeuchi, H. *J. Raman Spectrosc.*, **2002**, *33*, 530.
[57] Murakami-Kubo, I.; Doh-ura, K.; Ishikawa, K.; Kawatake, S.; Sasaki, K.; Kira, J.; Ohta, S.; Iwaki, T. *J. Virol.*, **2004**, *78*, 1281.

Bioorganic & Medicinal Chemistry 16 (2008) 6737–6746

Contents lists available at ScienceDirect

Bioorganic & Medicinal Chemistry

journal homepage: www.elsevier.com/locate/bmc

Antiprion activity of functionalized 9-aminoacridines related to quinacrine

Hanh Thuy Nguyen Thi [a], Chong-Yew Lee [a], Kenta Teruya [b], Wei-Yi Ong [c], Katsumi Doh-ura [b,*], Mei-Lin Go [a,*]

[a] Department of Pharmacy, National University of Singapore, 18 Science Drive 4, Singapore 117543, Singapore
[b] Department of Prion Research, Tohoku University Graduate School of Medicine, 2-1 Seiryo-cho, Aoba-ku, Sendai 980-8575, Japan
[c] Department of Anatomy, National University of Singapore, 18 Science Drive 4, Singapore 117543, Singapore

ARTICLE INFO

Article history:
Received 14 April 2008
Revised 27 May 2008
Accepted 28 May 2008
Available online 13 June 2008

Keywords:
Antiprion activity
6-Chloro-2-methoxy-(*N*⁹-substituted)acridin-9-amines
Quinacrine
Murine neuroblastoma cells infected with scrapie prion strains

ABSTRACT

A library of functionalized 6-chloro-2-methoxy-(*N*⁹-substituted)acridin-9-amines structurally related to quinacrine were synthesized and evaluated for antiprion activity on four different cell models persistently infected with scrapie prion strains (ScN2a, N167, Ch2) or a human disease prion strain (F3). Most of the compounds were distinguished by the side chain attached to 9-amino of the acridine ring. These were dialkylaminoalkyl and phenyl with basic groups on the phenyl ring. The most promising compound was 6-chloro-2-methoxy-*N*-(4-(4-methylpiperazin-1-yl)phenyl)acridin-9-amine (**15**) which had submicromolar EC_{50} values (0.1–0.7 μM) on all cell models, was able to clear PrP^{Sc} at non-toxic concentrations of 1.2–2.5 μM, and was more active than quinacrine in terms of EC_{50} values. Other promising compounds were **14** (a regioisomer of **15**) and **17** which had a 1-benzylpiperidin-4-yl substituent attached to the 9-amino function. Activity was strongly dependent on the presence of a substituted acridine ring, which in this library comprised 6-chloro-2-methoxy substituents on the acridine ring. The side chains of **14**, **15**, and **17** have not been previously associated with antiprion activity and are interesting leads for further optimization of antiprion activity.

1. Introduction

The transmissible spongiform encephalopathies (TSEs) or prion diseases are a group of infectious and fatal neurodegenerative diseases that include Creutzfeldt–Jakob disease (CJD) in humans, and scrapie, bovine spongiform encephalopathy, cervid chronic wasting disease among others, in animals.[1–4] These diseases may arise spontaneously, have a genetic origin or are acquired through infection. TSEs are characterized by the accumulation of protease-resistant aggregates of an altered isoform of the cellular prion protein (PrP^{C}) called scrapie prion protein (PrP^{Sc}) in the central nervous system and the lymphoreticular system. Unlike PrP^{C}, PrP^{Sc} has a multimeric structure with a high β sheet content. It can assemble into fibrils and plaques, a process that bears some similarity to the abnormal protein aggregation encountered in protein misfolding diseases such as Alzheimer's disease, Parkinson's disease, and Huntington's disease, except that PrP^{Sc} is also infectious. There is presently no clinically proven anti-TSE drug although significant progress has been made in identifying compounds with prophylactic activity.[5–7] Besides the general requirements of potency coupled with low toxicity, a successful antiprion drug must have good blood–brain permeability and the ability to halt or substantially modify pathogenesis late in the course of the disease.

Quinacrine, a 9-aminoacridine derivative, has been used for many years as an antimalarial agent.[8] It was found to inhibit PrP^{Sc} formation in a cell-based model of prion infection at submicromolar EC_{50} values,[9,10] but failed to demonstrate activity in scrapie-infected mice.[7,11,12] Nonetheless, it was used in a few patients with CJD on compassionate grounds, but was found to be only transiently beneficial in these cases.[13,14] In spite of these shortcomings, there is sustained interest in the antiprion activity of substituted 9-aminoacridines that are structurally related to quinacrine. May and co-workers[15] found bis-acridines like compound A (Fig. 1) to have more potent in vitro antiprion activity than quinacrine. Klingenstein and co-workers[16] observed the synergistic antiprion effects of quinacrine and iminodibenzyl-derived antidepressants, and this led to the synthesis of hybrid molecules like quinpramine and compound B (Fig. 1) which had 5- to 15-fold improved antiprion potencies over quinacrine in cell-based assays.[17] Investigations into the structure–activity relationships of quinacrine showed that antiprion activity was greatly influenced by several structural features, namely, the length of the alkyl linker attached to the 9-amino functionality, the substituents on the distal tertiary amino group of the alkyl side chain, and the substitution pattern on the acridine ring.[10,18]

* Corresponding authors. Tel.: +81 22 717 8232; fax: +81 22 717 7656 (K.D.); tel.: +65 65162654; fax: +65 67791554 (M.-L.G.).
E-mail addresses: doh-ura@mail.tains.tohoku.ac.jp (K. Doh-ura), phagoml@nus.edu.sg (M.-L. Go).

0968-0896/$ - see front matter © 2008 Elsevier Ltd. All rights reserved.
doi:10.1016/j.bmc.2008.05.060

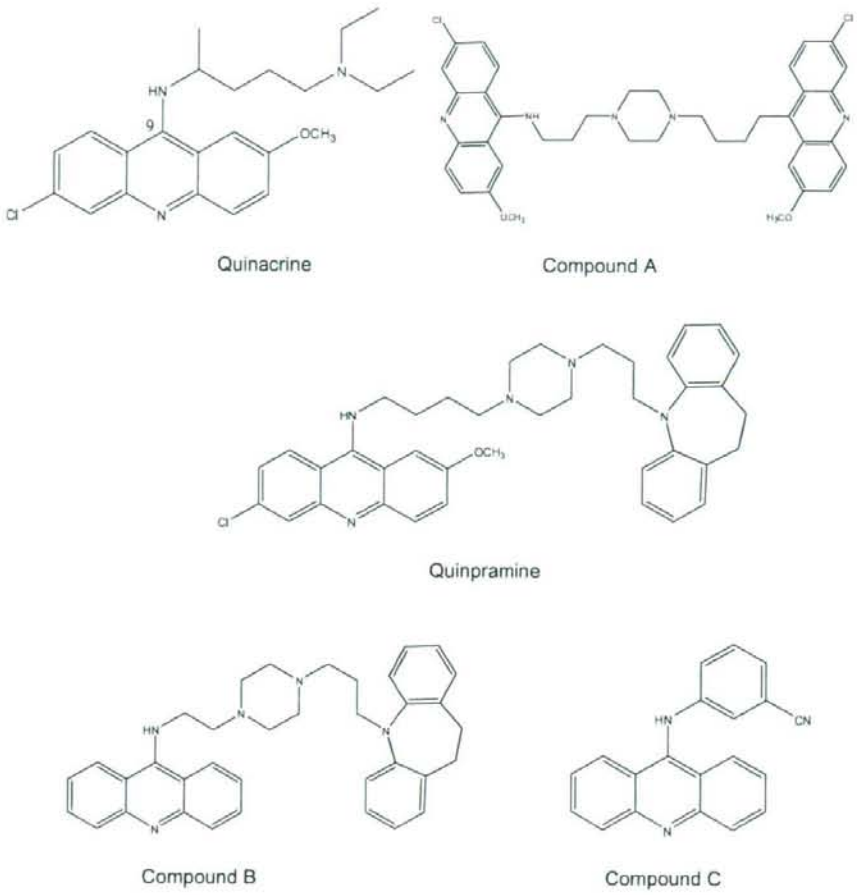

Figure 1. Structures of quinacrine and some antiprion acridines.

The latter feature was also identified as an important determinant of cellular cytotoxicity, with substituents like 3-fluoro-6-methoxy-4-methyl associated with greater cytotoxicity as compared to the 2-methoxy-6-chloro groups found on the acridine ring of quinacrine.[18] Cope and co-workers synthesized several substituted *N*-phenylacridin-9-amines and found electron withdrawing groups on the *N*-phenyl ring to be particularly favorable for activity. The most promising compound in their series (compound C, Fig. 1) had an EC_{50} of 1.0–2.5 μM on the scrapie mouse brain (SMB) cell model.[19] Taken together, these reports underscore the antiprion potential of the 9-aminoacridine template. For this reason, we have focused our medicinal chemistry efforts on 9-aminoacridines in an attempt to identify compounds with greater antiprion potencies and lower cytotoxicities than quinacrine. Here, we report the synthesis of a library of 6-chloro-2-methoxy-(*N*^{9}-substituted)acridine-9-amines and the evaluation of their antiprion activities on four different prion-infected cell models.

2. Chemistry

The synthesized compounds were broadly classified into four groups as shown in Table 1. The first group of compounds (**1–4**) were structurally related to quinacrine but with modifications on the side chain attached to the amino group at C^9 of the acridine ring, namely, the alkyl chain length between the nitrogen atoms of the side chain and the alkyl groups on the terminal nitrogen. Group 2 compounds (**5–16**) were 6-chloro-2-methoxy-*N*-phenyl acridin-9-amines, differentiated by the type of basic groups attached to the phenyl ring. These were *N*′,*N*′-dimethylamino, *N*′,*N*′-diethylamino, 1-piperidinyl, 1-pyrrolidinyl, 4-morpholinyl, and 4-methylpiperazin-1-yl, attached to 2′, 3′, or 4′ positions on the phenyl ring. Compounds with this motif have been associated with antimalarial, antitrypanosomal and cytotoxic activities,[20–22] but have not been widely investigated for antiprion activity. Group 3 consisted of miscellaneous compounds, namely, **17** which had a 1-benzylpiperidin-4-yl ring attached to the 9-amino functionality, **18** where the 9-amino functionality was part of the 4-methylpiperazin-1-yl ring, and **19** where a simple 9-amino group was present. Group 4 comprised only two compounds (**20, 21**) with unsubstituted acridine rings, in contrast to Groups 1–3 compounds which had 6-chloro-2-methoxy substituents. Compounds **20** and **21** are the unsubstituted equivalents of compounds **9** and **19**, respectively, and a comparison of their activities would provide some useful information on the role of ring substitution for activity.

Table 1
Antiprion activity of quinacrine and library compounds on ScN2a cells

Compound	Substituent	EC_{50} (μM)[a]	FAA (μM)[b]	TC (μM)[c]	SI[d]
	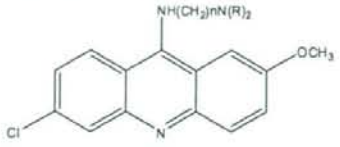 Group1				
1	$n = 2$, R = C_2H_5	0.021 (0.019–0.023)	0.1	4	190
2	$n = 3$, R = C_2H_5	0.14 (0.11–0.17)	0.3	1	7
3	$n = 4$, R = C_2H_5	0.15 (0.12–0.19)	0.4	1	7
4	$n = 3$, R = CH_3	0.11 (0.09–0.13)	0.3	1	9
	Quinacrine	0.23 (0.22–0.25)	0.8	2.5	11
	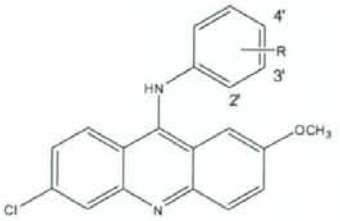 Group 2				
5	2'-$N(CH_3)_2$	0.25 (0.22–0.28)	0.8	5	20
6	3'-$N(CH_3)_2$	0.32 (0.26–0.39)	None[e]	2	6
7	4'-$N(CH_3)_2$	0.51 (0.34–0.77)	None[e]	2	4
8	3'-$N(C_2H_5)_2$	1.01 (0.85–1.21)	2.5	3	3
9	4'-$N(C_2H_5)_2$	0.48 (0.24–0.93)	1.5	2	4
10	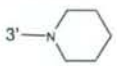	0.18 (0.15–0.22)	0.5	4	22
11	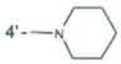	4.24 (3.67–4.90)	7	9	2
12	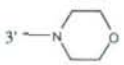	0.9 (0.75–1.08)	None[e]	3	3
13	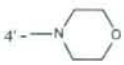	1.28 (1.16–1.42)	3	4	3
14	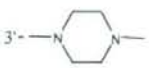	0.29 (0.26–0.33)	1	4	14
15	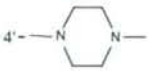	0.1 (0.08–0.12)	0.4	2.5	25
16		1.06 (0.95–1.18)	None[e]	2	2
	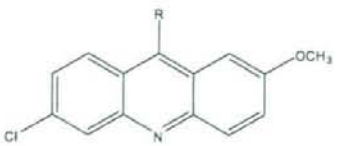 Group 3				

(continued on next page)

Table 1 (*continued*)

Compound	Substituent	EC_{50} (μM)[a]	FAA (μM)[b]	TC (μM)[c]	SI[d]
17	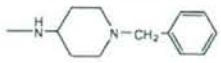	0.42 (0.38–0.46)	1	2	5
18	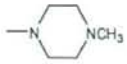	0.36 (0.29–0.45)	1.8	4	11
19	$-NH_2$	0.13 (0.12–0.14)	0.4	4	30
	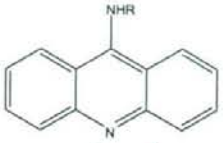 Group 4				
20		0.24 (0.16–0.36)	None[e]	0.4	2
21[f]	H	None[e]	None[e]	2.5	–

[a] Concentration required to reduce PrP^{Sc} content to 50% of untreated ScN2a cells, average of no less than three independent determinations. 95% Confidence intervals are given in brackets.
[b] Full antiprion activity: estimated lowest concentration required for more than 99% reduction of PrP^{Sc}.
[c] Tolerant concentration: estimated maximal concentration that had no toxic effect on cell growth to confluency.
[d] Selectivity index = TC/EC_{50}.
[e] Could not be determined at non-toxic concentrations of test compound.
[f] Purchased from Sigma-Aldrich Chemical Company.

The target compounds were synthesized by the selective displacement of the chlorine atom at position 9 of 6,9-dichloro-2-methoxyacridine by a nucleophilic primary amine (Scheme 1). The reaction was carried out in ethanol under weakly acidic conditions. The displacement reaction occurred only at C^9 and not at C^6, because of the proximity of C^9 to the electron withdrawing acridinium nitrogen as well as the stability of the resulting intermediate. Phenol has been employed as solvent, in which case a phenoxide intermediate was formed in situ and subsequently displaced by the incoming amine.[23,24] In our hands, both solvents gave comparable yields but workup procedures were generally easier with ethanol. In cases where yields in ethanol were unsatisfactory, a change to phenol provided a favorable solution.

Many of the amines used in the condensation reaction were prepared from iodobenzene in a palladium-coupled Hartwig–Buchwald amination reaction (Scheme 2). 4-(3-Nitrophenyl)morpholine, 1-methyl-4-(3-nitrophenyl)piperazine (and its 4-isomer), 1-(3-nitrophenyl)piperidine, 1-(3-nitrophenyl)pyrrolidine, and *N*′,*N*′-dimethyl-3-nitroaniline were obtained in this way in fairly good yields. The aromatic nitro function of these compounds was subsequently reduced by palladium catalyzed hydrogenation to give the desired aniline which was subsequently reacted with the 4,6-dichloro-2-methoxyacridine as shown in Scheme 1. A different

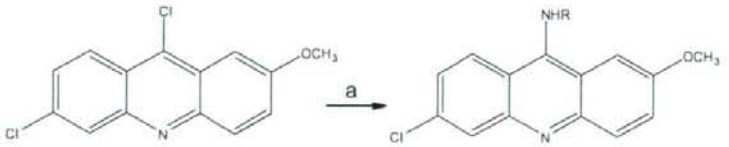

Scheme 1. Reagents and conditions: (a) RNH_2, ethanol, HCl, reflux, 24 h or phenol, 100 °C (1 h), followed by addition of amine, 4–5 h, 100 °C.

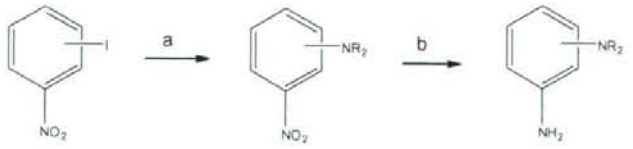

Scheme 2. Reagents and conditions: (a) Amine (pyrrolidine, piperidine, 1-methylpiperazine, morpholine, or *N*,*N*-dimethylamine), $Pd(OAc)_2$, BINAP, Cs_2CO_3, anhydrous toluene, 120 °C; (b) H_2, 10% Pd/C (5% w/w), 50 psi.

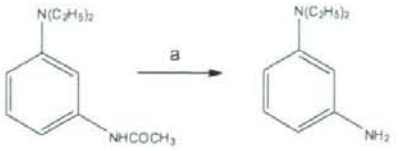

Scheme 3. Reagent and conditions: (a) Concd HCl, reflux, 2 h.

route was adopted for N^1,N^1-diethylbenzene-1,3-diamine, which was prepared from the acid hydrolysis of the commercially available *N*-(3-(diethylamino)phenyl)acetamide (Scheme 3). N^1,N^1-Dimethylbenzene-1,2-diamine was prepared by reacting 1-chloro-2-nitrobenzene with hexamethylphosphoramide (HMPA), followed by catalytic reduction of the aromatic nitro group (Scheme 4).

3. Results

3.1. Antiprion activity against ScN2a cells

ScN2a cells are murine neuroblastoma cells (N2a) that have been persistently infected with the scrapie prion strain RML. This cell model is widely used for the screening of antiprion candidates, resulting in the identification of several promising target compounds like acridines and phenothiazines,[10] chrysoidine,[25] and quinoline derivatives.[26,27] The method involved incubating the test compound with the ScN2a cells until confluency was attained (3 days), after which the cells were lysed to give lysates that were treated with proteinase K and analyzed by immunoblot for PrP immunoreactivity. PrP^{Sc} is resistant to proteinase K digestion and shows characteristic bands in the immunoblot. The signal levels of these bands are reduced in the presence of a compound with antiprion activity. Figure 2 shows the results of representative immunoblots obtained at different concentrations (0.1–2.0 μM) of compound **15**.

EC_{50} which is the effective concentration of test compound required to reduce PrP^{Sc} content to 50% of untreated ScN2a cells was determined by measuring the intensities of the immunoreactive signals at different concentrations of test compound. The results were plotted to give a sigmoidal curve from which EC_{50} was obtained. A representative plot is given in Figure 3.

Table 1 lists the antiprion effects of the test compounds expressed in terms of their (i) EC_{50} values, (ii) full antiprion activity (FAA) which is the approximate concentration required to clear more than 99% of PrP^{Sc} content, and (iii) maximal tolerant concentration (TC) which is the approximate highest concentration to have no toxic effect on uninfected N2a cells. The ratio of the

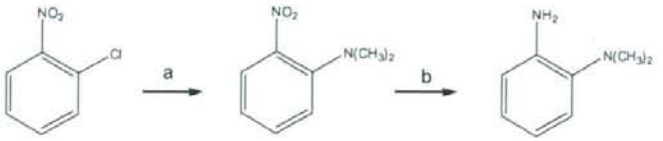

Scheme 4. Reagents and conditions: (a) Hexamethylphosphoramide, 150 °C, 24 h; (b) H_2, 10% Pd/C (5% w/w), 50 psi.

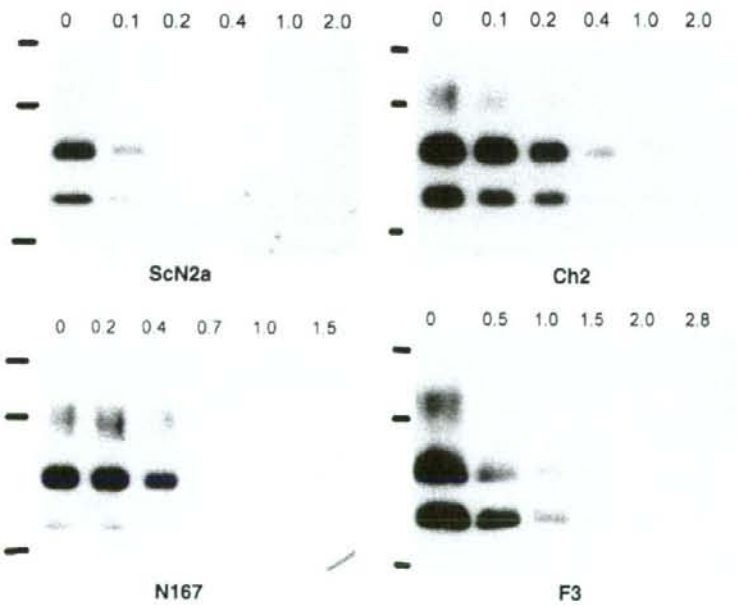

Figure 2. Immunoblots of PrP^{Sc} formation in the presence of compound **15** in ScN2a, Ch2, N167 and F3 prion-infected cell models. Apparent molecular masses based on migration of protein standards are 45.7, 32.5 and 18.4 kDa (from top to bottom). The top most line in each panel gives the concentration (μM) of **15**. The first column on the right ('0') represents cells that were not treated with **15**.

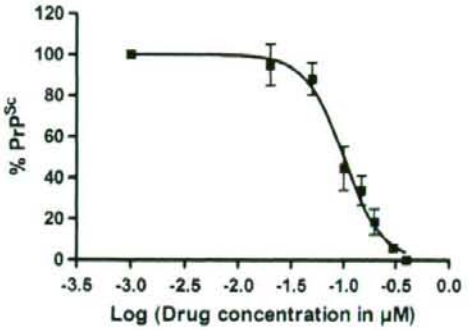

Figure 3. Plot of % PrP^{Sc} formation (equivalent to intensities of immunoreactive signals relative to untreated cells) in ScN2a cells treated with different concentrations of compound **15**. EC_{50} was obtained from the descending portion of the sigmoidal curve using a commercial software program GraphPad Prism 4.03.

tolerant concentration (TC) to EC_{50} gives the selectivity index, which is a useful measure of the selective activity of the compound.

Quinacrine was used as the reference compound in these experiments. Its EC_{50} was found to be 0.23 μM. This value compares favorably with those reported by others like Doh-ura et al.[9] (EC_{50} 0.4 μM under similar experimental conditions) and Dollinger et al.[17] (EC_{50} 0.3 μM, incubation period of 7 days).

As seen from Table 1, many compounds had submicromolar EC_{50} values that were comparable to quinacrine. Compound **1** was particularly interesting because of its potency (EC_{50} 0.021 μM, almost 10 times lower than quinacrine) and exceptionally high selectivity index (SI = 190). The activity of **1** was found to be sensitive to the length of the side chain separating the two amino functions in the side chain. In **1**, the amino functions are separated by two carbon atoms ($n = 2$). As more carbon atoms were introduced, activity and selectivity declined, as seen from its homologues, compounds **2** ($n = 3$) and **3** ($n = 4$). On the other hand, activity was less affected by the type of substituents on the distal amino function. Thus for the same alkyl chain length ($n = 3$), no difference in activity was noted for compounds **2** (N',N'-diethylamino) and **3** (N',N'-dimethylamino).

The Group 2 compounds were *N*-phenylacridin-9-amines with different basic substituents attached to the *N*-phenyl ring. A cursory examination of antiprion activity in this Group (Table 1) suggests that among the basic heterocycles attached to the *N*-phenyl ring, the 1-methylpiperazine ring present in compounds **14** and **15** was preferred to other basic rings like piperidine (**10, 11**), pyrrolidine (**16**), or morpholine (**12, 13**). Mention should also be made of compounds **5, 10**, and **15** which had significantly good selectivities (SI ≥ 20) compared to quinacrine (SI = 11) but EC_{50} values (0.1–0.25 μM) that were just comparable to quinacrine (0.23 μM).

The antiprion activities of the Group 3 compounds **17** and **18** were broadly similar to most members in Group 2. Thus we inferred that the substitution of the 9-amino functionality with phenyl (Group 2) or a non-aromatic heterocyclic ring (Group 3, namely **17, 18**) did not markedly affect antiprion activity. The activity of compound **19** which has an unsubstituted 9-amino functionality was unexpectedly good (EC_{50} 0.13 μM, SI = 30), in sharp contrast to its ring-unsubstituted analogue **21** (9-aminoacridine) which was the only compound in the entire library with no detectable activity on ScN2a cells. Another ring-unsubstituted compound **20** was also found to have a poor antiprion profile, providing additional support to the view that an unsubstituted acridine ring was detrimental to activity.

3.2. Antiprion activity against other prion-infected cell models

Besides ScN2a, the compounds were also evaluated on other prion-infected cell models as described in previous studies.[28,29] These were N167 which were mouse neuroblastoma cells (N2a) infected with the scrapie prion strain 22L, and Ch2 which were mouse neuroblastoma cells (N2a#58) that overexpressed PrP^{C} (3–5 times more than N2a cells) and infected with the scrapie prion strain RML. The third cell model F3 was N2a#58 cells infected with the mouse-adapted human prion strain Fukuoka-1. Only some compounds were screened against these additional cell models and they were chosen based on their selectivity indices (SI) compared to quinacrine in ScN2a cells: **1, 15**, and **19** had better selectivities (SI > 20), **14** and **18** were comparable to quinacrine, while **11** and **17** had poorer selectivities (SI < 10). The antiprion activities of these compounds are given in Table 2.

Table 2 clearly shows that antiprion activity varied according to the cell model employed for testing. On the N167 cells, compounds **1** and **19** had no measurable EC_{50} values, in contrast to their strong antiprion activities against ScN2a cells. The most promising compounds on the N167 cell model (**15** and **17**) were also not particularly outstanding against ScN2a cells. On the N167 model, **15** and **17** had EC_{50} values (0.42 and 0.49 μM) that were comparable to quinacrine (0.59 μM) but they were able to clear PrP^{Sc} at 1.5 μM, a feature that was not observed for quinacrine.

A comparison of EC_{50} values against Ch2 and ScN2a showed that most compounds were less potent against the PrP^{C} overexpressing Ch2 cell model. A notable exception was **17** which retained the same level of activity (EC_{50} 0.4 μM) on both Ch2 and ScN2a. Compounds **14** and **15** were also interesting in that they were

Table 2
Antiprion activities of quinacrine and selected compounds against different prion-infected cell lines

Compound	Prion-infected cell lines							
	ScN2a		N167		Ch2		F3	
	EC_{50}[a]	FAA[b]	EC_{50}[a]	FAA[b]	EC_{50}[a]	FAA[b]	EC_{50}[a]	FAA[b]
1	0.021	0.1	None[c]	None[c]	0.7 *(0.41–1.19)*	3	None[c]	
11	4.24	7	4.29 *(3.90–4.73)*	None[c]	None[c]	ND[d]	ND[d]	ND[d]
14	0.20	1	1.19 *(0.92–1.53)*	3	0.38 *(0.31–0.48)*	1.5	1.49 *(1.34–1.65)*	3.5
15	0.10	0.4	0.42 *(0.41–0.43)*	1.5	0.22 *(0.19–0.27)*	1.2	0.68 *(0.59–0.78)*	1.5
17	0.42	1	0.49 *(0.49–0.55)*	1.5	0.41 *(0.32–0.51)*	1	0.80 *(0.64–1.00)*	None[c]
18	0.36	1.8	None[c]	None[c]	>2	ND[d]	None[c]	None[c]
19	0.13	0.4	None[c]	None[c]	None[c]	None[c]	ND[d]	ND[d]
Quinacrine	0.23	0.8	0.59 *(0.42–0.82)*	None[c]	0.46 *(0.40–0.54)*	2	1.88 *(1.64–1.00)*	None[c]

[a] Concentration (μM) required to reduce PrP^{Sc} content to 50% of untreated cells from three independent determinations. 95% confidence limits are given in italics.
[b] Full antiprion activity: estimated lowest concentration (μM) required for more than 99% reduction of PrP^{Sc}.
[c] No data were obtained at non-toxic concentrations.
[d] Not determined.

more active (lower EC_{50} and FAA values) than quinacrine on the Ch2 cell model.

The compounds were also tested on the F3 cells which are PrP^C over-producing mouse neuroblastoma cells (N2a#58) infected with a mouse-adapted human prion strain. Here, only quinacrine **14**, **15**, and **17** retained antiprion activity, but with EC_{50} values that were 2- to 5-fold higher than those determined against Ch2 cells. Potency measured in terms of EC_{50} was of the order **15** (0.68 μM) > **17** (0.80 μM) > **14** (1.49 μM) > quinacrine (1.88 μM). Only **14** and **15** were able to clear the cells of PrP^{Sc} formation.

4. Discussion

Based on the screening results given in Tables 1 and 2, compounds **14**, **15**, and **17** were found to be the most promising candidates. These compounds had measurable EC_{50} values in the low to submicromolar range on four different prion cell models that were persistently infected with scrapie prion strains (ScN2a, N167, Ch2) or a human disease prion strain (F3). In addition, they were able to clear PrP^{Sc} formation at low micromolar concentrations, except for **17** against F3 cells. These compounds were either comparable or more active than quinacrine on most of these cell models.

The antiprion profile of compound **15** was of particular interest because its activity was restricted to a narrow EC_{50} range (0.1–0.7 μM). It had a good selective index of 25 and was able to clear PrP^{Sc} formation at FAA values of about 1.5 μM. In addition, its antiprion activity appears to be better than that of quinacrine on all four cell models. Structurally, **15** is *N*-phenylacridin-9-amine with a (4-methylpiperazin-1-yl) ring attached to the 4′ position of the phenyl ring. Some structure–activity trends may be deduced for **15**. First, relocating 4-methylpiperazin-1-yl from 4′ to 3′ gave **14**, another promising compound which retained activity on all prion-infected cell models but at higher EC_{50} and FAA values than **15**. Second, replacing 4-methylpiperazin-1-yl in **15** with piperidin-1-yl gave **11**, which had sharply reduced activity on ScN2a and N167 cells. Another observation was that bypassing the phenyl ring and directly linking the 4-methylpiperazine ring to acridine, as in **18**, adversely affected activity. Lastly, the results from ScN2a cells indicated that 4-methylpiperazin-1-yl was the preferred substituent, compared to other basic moieties like piperidin-1-yl, morpholin-1-yl and pyrrolidin-1-yl. Taken together, these observations underscore the antiprion potential of appropriately substituted *N*-phenylacridine-9-amines, as exemplified by **14** and **15**. Compound **15** in particular has a promising antiprion profile which warrants further investigation.

The antiprion activities of other *N*-phenylacridin-9-amines have been reported earlier by Cope and co-workers,[19] but they were tested on a different cell model (SMB) which makes comparison with the present results difficult. Nonetheless, it was noted that one compound in their study (**1o**, N^1-(acridin-9-yl) benzene-1,3-diamine) which had a primary amino function on the phenyl ring did not fare as well as other compounds in their library. If we extrapolate from our present SAR, activity of **1o** may be improved by introducing substituents on the acridine ring or by having a bulkier basic group like tertiary amine or a basic heterocycle on the phenyl ring. As we have shown, compounds **20** and 21 with no substituents on the acridine ring did not fare as well as their ring substituted analogues (**9** and **19**), and the most promising compounds in our library (**14**, **15**, **17**) have tertiary substituted amino groups.

Mention should also be made of compound **17** which was not particularly active against ScN2a (EC_{50} 0.42 μM) and had a low selectivity index (5). In spite of these limitations, **17** retained the same level of activity against N167 and Ch2 cells (EC_{50} 0.41–0.49 μM) which was in contrast to quinacrine, **14** and **15**, which had lower activities against N167 and Ch2 cells. Compound **17** was also active against the mouse-adapted human prion strain Fukuoka-1 (EC_{50} 0.8 μM) but failed to clear PrP^{Sc} formation in this cell model. Structurally, **17** has a 1-benzylpiperidin-4-yl side chain attached to the 9-amino of acridine and this entity has not been previously associated with antiprion activity. It would be of interest to see if structural modifications of this side chain could overcome some of the limitations associated with **17**.

5. Conclusions

We have shown that structural modification of the 9-substituted amino side chain of quinacrine resulted in several promising compounds (**14**, **15**, and **17**) with good antiprion potencies and selectivities on four prion-infected murine cell models, including a mouse-adapted human prion strain (F3). Compounds **14** and **15** are 6-chloro-2-methoxy-(*N*-substituted)phenylacridin-9-amines with 4-methyl piperazin-1-yl side chains attached to different positions on the phenyl ring. In compound **17**, the 9-amino functionality of 6-chloro-2-methoxy-9-aminoacridine is substituted with 1-benzylpiperidin-4-yl. Both basic side chains have not been previously associated with antiprion activity and are interesting leads for further modification. Further investigations would involve evaluating their activities in vivo, and to assess their permeability across the blood–brain barrier.

6. Experimental

6.1. Chemistry

Melting points were determined in open glass capillary tubes on a Gallenkamp melting point apparatus and were not corrected. ^1H NMR and ^{13}C NMR spectra were recorded on a Bruker DPX 300 MHz spectrometer and chemical shifts were reported in δ (ppm) relative to the internal standard TMS. Mass spectra were collected on LCQ Finnigan MAT mass spectrometer with chemical ionization (APCI) or electron spray ionization (ESI) as probes. Reactions were routinely monitored by thin layer chromatography using silica gel 60 F 254 plates from Merck, with UV light as a visualizing agent. Column chromatography was performed using silica gel G (0.04–0.063 mm) from Merck. The purity of final compounds was verified by high pressure liquid chromatography (HPLC) (Supplementary information) or by combustion analysis. Combustion analyses (C,H) were determined by Perkin-Elmer PE 2400 CHN/CHNS elemental analyzer by the Department of Chemistry, National University of Singapore.

All chemicals were purchased from Sigma–Aldrich Chemical Company (MO, USA), except piperidine and *N,N*-dimethyl-3-nitroaniline, which were purchased from Tokyo Chemical Industry (Tokyo, Japan) and Alfa Aesar (MA, USA), respectively.

6.1.1. General procedure for Hartwig–Buchwald amination

1-Iodo-3 (or 4)-nitrobenzene (2.49 g, 10 mmol) and the amine (1-methylpiperazine, pyrrolidine, piperidine, morpholine) (25 mmol) were dissolved in dry toluene (30–50 ml) in the presence of argon in a round-bottomed flask. The solution was transferred via a canula under positive pressure to another flask which contained cesium carbonate (8.15 g, 25 mmol) and *rac*-BINAP (rac-2,2′-bis(diphenylphosphino)-1,1′-binaphthyl) (0.50 g, 0.8 mmol), which were earlier weighed into the flask in the presence of argon. $Pd(OAc)_2$ (palladium (II) acetate) (0.013 g, 0.06 mmol) was quickly added to the flask and the reaction mixture was heated to 90 °C in an oil bath, with stirring. The reaction was stopped when traces of the iodonitrobenzene were not

observed on TLC. After cooling to room temperature, the mixture was filtered and the organic phase concentrated under reduced pressure. The residue was purified by column chromatography using as mobile phase ethylacetate/hexane (1:1) which was increased stepwise to ethyl acetate/methanol/ammonia (9:1:0.1).

6.1.1.1. 4-(3-Nitrophenyl)morpholine. Orange solid. Yield 80%. ^{1}H NMR (300 MHz, $CDCl_3$) δ 3.25 (t, 4H, J = 5.3) 3.89 (t, 4H, J = 5.3), 7.18 (dd, $J1$ = 1.9, $J2$ = 8.4, 1H) 7.40 (t, J = 8.1, 1H) 7.71 (m, 2H).

6.1.1.2. 1-Methyl-4-(3-nitrophenyl)piperazine. Red solid. Yield 92%. ^{1}H NMR (300 MHz, $CDCl_3$) δ 2.30 (s, 3H) 2.58 (t, J = 5.3, 4H) 3.30 (t, J = 5.3, 4H) 7.37 (m, 2H) 7.66 (m, 2H).

6.1.1.3. 1-Methyl-4-(4-nitrophenyl)piperazine. Red solid. Yield 95%. ^{1}H NMR (300 MHz, $CDCl_3$) δ 2.36 (s, 3H) 2.56 (t, J = 4.3, 4H) 3.44 (t, J = 4.3, 4H) 6.83 (d, J = 9.4, 2H) 8.13 (d, J = 9.4, 2H).

6.1.1.4. 1-(3-Nitrophenyl)pyrrolidine. Orange solid. Yield 85%. ^{1}H NMR (300 MHz, $CDCl_3$) δ (ppm) 2.06 (t, J = 6.6, 4H) 3.34 (t, J = 6.6, 4H) 6.80 (dd, $J1$ = 2.1, $J2$ = 8.0, 1H) 7.32 (m, 2H) 7.46 (dd, $J1$ = 1.7, $J2$ = 8.0, 1H). MS (ESI, MeOH) m/z [M+1]$^+$ 193.4.

6.1.1.5. 1-(3-Nitrophenyl)piperidine. Orange liquid. Yield 80%. ^{1}H NMR (300 MHz, $CDCl_3$) δ (ppm) 1.64 (m, 2H) 1.72 (m, 4H) 3.27 (t, J = 5.3, 4H) 7.18 (dd, $J1$ = 2.3, $J2$ = 8.3, 1H) 7.34 (t, $J1$ = 2.3, $J2$ = 8.3, 1H) 7.60 (dd, $J1$ = 1.6, $J2$ = 8.0, 1H) 7.71 (t, J = 2.1, 1H). MS (ESI, MeOH) m/z [M+1]$^+$ 207.3.

6.1.2. N^1,N^1-Dimethyl-2-nitrobenzene

Hexamethylphosphoramide (2.69 g, 15 mmol, 2.5 ml) was added to 1-chloro-2-nitrobenzene (0.4 g, 2.5 mmol) in a flask under argon and heated at 150 °C for 24 h. The reaction mixture was diluted with water (≈20 ml), extracted with ether, after which the ether fraction was extracted with 4 M HCl (4× 10 ml). The acidic fraction was made alkaline with 4 M NaOH, extracted with ether (4× 20 ml), and dried over anhydrous Na_2SO_4. After removal of ether under reduced pressure, the residue was recrystallised in ethanol to give yellow crystals. Yield 40%. ^{1}H NMR ($CDCl_3$) δ 3.09 (s, 6H) 7.10 (d, J = 1.5, 1H) 7.57 (d, J = 1.5, 1H) 7.88 (s, 1H).

6.1.3. General procedure for catalytic reduction of the aromatic nitro functionality

The nitrobenzene was dissolved in ethanol and the catalyst (10% palladium on carbon) (5% w/w) was added under nitrogen. Hydrogenation was carried out on a Parr hydrogenator at 50 psi for 12–18 h. At the end of the process, the catalyst was removed by filtration and the filtrate is concentrated in vacuo. The product was obtained quantitatively and used immediately for the next step of reaction.

6.1.4. General procedure for the reaction of 6,9-dichloro-2-methoxyacridine with amines in phenol

This method was used for the syntheses of **1–5, 8, 9, 17, and 18**. 9-Dichloro-2-methoxyacridine (0.28 g, 1 mmol) was added to melted phenol (0.94 g, 10 mmol) and stirred at 100 °C for 1 h before addition of the amine (1.1 mmol). Stirring was continued for 3–4 h at 120 °C under nitrogen. On cooling to room temperature, diethylether was added to the reaction mixture. The resulting precipitate was either removed by vacuum filtration or extracted with dichloromethane. It was dissolved in an appropriate solvent and purified by column chromatography. The final compound was recrystallized from methanol or converted to a HCl salt with ethereal HCl.

6.1.5. N^1-(6-Chloro-2-methoxyacridin-9-yl)-N^2,N^2-diethylethane-1,2-diamine dihydrochloride (1)

6,9-Dichloro-2-ethoxyacridine and N^1,N^1-diethylethane-1,2-diamine were reacted in phenol to give **1** as a yellow solid in 74% yield. Mp 252–254 °C (lit. 257–259 °C). ^{1}H NMR (CD_3OD) δ 1.41 (t, J = 7.2, 6H) 3.39 (q, J = 7.2, 4H) 3.80 (t, J = 6.4, 2H) 4.06 (s, 3H) 4.63 (t, J = 6.4, 2H) 7.55 (dd, $J1$ = 2.7, $J2$ = 9.3, 1H) 7.67 (t, J = 8.3, 1H) 7.80 (dd, $J1$ = 4.2, $J2$ = 9.2, 1H) 7.86 (d, J = 2.7, 1H) 8.01 (d, J = 3.0, 1H) 8.49 (dd, $J1$ = 1.5, $J2$ = 9.4, 1H). MS (ESI, MeOH) m/z [M$^+$] 358.1. Anal. ($C_{20}H_{24}N_3OCl.2HCl.H_2O$) C calcd 53.51, found 53.33; H calcd 6.24, found 6.03.

6.1.6. N^1-(6-Chloro-2-methoxyacridin-9-yl)-N^3,N^3-diethylbenzene-1,3-diamine (8)

3-(*N*,*N*-Diethylamino)acetanilide (1.2 g, 5.8 mmol) and 2.5 ml concentrated HCl were heated to 100 °C for 2 h. On cooling, the pH of the solution was adjusted to 4 with 2 M NaOH. The product, N^1,N^1-diethylbenzene-1,3-diamine, was not isolated or purified but directly reacted with 6,9-dichloro-2-methoxyacridine (1.61 g, 5.8 mmol) in phenol as described under the general procedure. The product was obtained as an orange solid in 41% yield and was converted to the HCl salt with ethereal HCl. Mp 274–276 °C. ^{1}H NMR (CD_3OD) δ 1.10 (t, J = 7.0, 6H) 3.38 (q, J = 7.0, 4H) 3.67 (s, 3H) 6.63 (d, J = 7.7, 1H) 6.69 (t, J = 2.0, 1H) 6.79 (dd, $J1$ = 2.3, $J2$ = 8.5, 1H) 7.33 (t, J = 8.1, 1H) 7.41 (dd, $J1$ = 2.0, $J2$ = 9.4, 1H) 7.56 (d, J = 2.5, 1H) 7.64 (dd, $J1$ = 2.6, $J2$ = 9.3, 1H) 7.82 (d, J = 9.3, 1H) 7.88 (d, J = 1.9, 1H) 8.25 (d, J = 9.4, 1H). MS (ESI, MeOH) m/z [M$^+$] 406.3. Anal. ($C_{24}H_{24}N_3OCl.HCl.1/4H_2O$) C calcd 64.50, found 64.56; H calcd 5.64, found 5.79.

6.1.7. N^6-(1-Benzylpiperidin-4-yl)-6-chloro-2-methoxyacridin-9-amine (17)

Compound **17** was obtained as a yellow solid in 48% yield. Mp 136–138 °C ^{1}H NMR ($CDCl_3$) δ 1.74 (d, J = 9.4, 2H), 2.05 (t, J = 9.4, 4H), 2.90 (d, J = 11.7, 2H), 3.51 (s, 2H), 3.70 (b, 1H), 3.96 (s, 3H), 4.34 (b, 1H), 7.19 (d, J = 2.5, 1H), 7.30 (m, 4H), 7.34 (d, J = 2.1, 1H) 7.37 (d, J = 2.0, 1H), 7.44 (dd, $J1$ = 2.6, $J2$ = 9.4, 1H), 8.01 (t, J = 9.5, 2H), 8.10 (d, J = 1.8, 1H). MS (ESI, MeOH) m/z [M$^+$] 432.4.

6.1.8. General procedure for the reaction of 6,9-dichloro-2-methoxyacridine with amines in ethanol

This method was used for the preparation of compounds **6, 7, 10–16, 19, and 20**. 6,9-Dichloro-2-methoxyacridine (2 mmol) and the reacting amine (0.56 g, 2 mmol) were dissolved in ethanol (30–50 ml) and 2 drops of concentrated HCl were added. The mixture was refluxed and the course of reaction followed by TLC until little or no starting material was detected (around 24 h). On cooling to room temperature, the reaction mixture was diluted with cold water and neutralized with 28% v/v ammonia solution. The precipitate was collected by vacuum filtration, washed with distilled water, and purified by column chromatography (gradient elution with ethyl acetate/hexane 1:1 to ethyl acetate/methanol/ammonia 9:1:0.1). If neutralization (with ammonia or 1 M NaOH) did not result in precipitation of the desired product, the alkaline solution was extracted with dichloromethane. The organic layer was washed with brine, concentrated in vacuo, and purified by column chromatography.

6.1.9. 6-Chloro-2-methoxy-*N*-(3-(4-methylpiperazin-1-yl)phenyl)acridin-9-amine (14)

6,9-Dichloro-2-methoxyacridine and 3-(4-methylpiperazin-1-yl)aniline (obtained from reduction of 1-methyl-4-(3-nitrophenyl)piperazine) were reacted in ethanol to give **14** as a red solid in 72% yield. Decomposed at 114 °C. ^{1}H NMR ($CDCl_3$) δ 2.32 (s, 3H), 2.50 (t, J = 4.4, 4H), 3.11 (t, J = 4.5, 4H), 3.78 (s, 3H), 6.30 (d, J = 7.6, 1H), 6.40 (s, 1H), 6.43 (s, 1H), 6.55 (d, J = 8.3, 1H), 7.13 (d, J = 5.8,

2H), 7.44 (d, J = 10.3, 1H), 7.98 (d, J = 8.9, 1H), 8.07 (d, J = 9.0, 1H), 8.17 (s, 1H). MS (ESI, MeOH) m/z [M$^+$] 433.2.

6.1.10. 6-Chloro-2-methoxy-*N*-(4-(4-methylpiperazin-1-yl)phenyl)acridin-9-amine (15)

6,9-Dichloro-2-methoxyacridine and 4-(4-methylpiperazin-1-yl)aniline (obtained from reduction of 1-methyl-4-(4-nitrophenyl)piperazine) were reacted in ethanol to give **15** as a yellow solid in 65% yield. Mp 190.9–192.2 °C. ^{1}H NMR ($CDCl_3$) δ 2.33 (s, 3H), 2.56 (t, J = 4.8, 4H), 3.12 (t, J = 4.6, 4H), 3.66 (s, 3H), 6.82 (b, 4H), 7.08 (s, 1H), 7.15 (d, J = 9.1, 1H), 7.32 (d, J = 9.4, 1H), 7.85 (d, J = 9.2, 1H), 7.94 (d, J = 9.0, 1H), 8.02 (s, 1H). MS (ESI, MeOH) m/z [M$^+$] 431.9.

6.1.11. 6-Chloro-2-methoxyacridin-9-amine dihydrochloride (19)

6,9-Dichloro-2-methoxyacridine (0.028 g, 0.1 mol) was dissolved in 200 ml of methanol and refluxed for 2 h with a solution of sodium methoxide, prepared by dissolving sodium (0.003 g, 0.12 mol) in 50 ml of methanol. The precipitated sodium chloride was removed by filtration and the filtrate treated with water to precipitate the desired product. ^{1}H NMR (300 MHz, $CDCl_3$) δ 4.01 (s, 3H) 4.21 (s, 3H) 7.38 (d, J = 2.7, 1H) 7.47 (m, 2H) 8.09 (d, J = 9.5, 1H) 8.19 (m, 2H). The product, 6-chloro-2,9-dimethoxyacridine, was dissolved in 20 ml of alcohol and treated with ammonium chloride (0.64 g, 0.12 mol) dissolved in 2 ml of water. The mixture was maintained at 60–70 °C for 2 h. Compound **19** was obtained as a yellow solid by filtration. (85% yield). Mp 341 °C. ^{1}H NMR (300 MHz, CD_3OH) δ 8.71–7.20 (m, 6H), 3.96 (s, 3H). MS (ESI, MeOH) m/z [M]$^+$ 258.1.

6.1.12. N^1-(Acridin-9-yl)-N^4,N^4-diethylbenzene-1,4-diamine (20)

6,9-Dichloro-2-methoxyacridine and N^1,N^1-diethylbenzene-1,4-diamine were reacted in ethanol as described in the general procedure. Product was obtained as a brownish red solid in 88% yield. Mp 227–228 °C. ^{1}H NMR ($CDCl_3$) δ 1.09 (t, J = 6 Hz, 6H) 3.25 (q, J = 6 Hz, 4H) 6.56 (d, J = 9 Hz, 2H) 6.84 (d, J = 9 Hz, 2H) 7.21–7.16 (m, 2H) 7.57 (t, J = 9 Hz, 2H) 7.94 (t, J = 9 Hz, 4H). MS (ESI, MeOH) m/z [M$^+$] 341.2.

6.2. Antiprion activity assay

The assay was performed as described previously.[26,28,29] Briefly, the ScN2a, N167, Ch2, and F3 cells were grown in minimal essential medium (Opti-MEM, Invitrogen) supplemented with 10% fetal calf serum. Approximately 2 × 10^6 cells were seeded into each well of a six-well plate. Stock solutions of the test compounds were prepared in DMSO and were added to the wells when cells were seeded. The final concentration of DMSO in each well was kept at <0.5% v/v. When the cells reached confluency after 3 days, they were examined microscopically (10× magnification) for signs of abnormal appearances. The medium was then removed from each well by aspiration, the cells were rinsed with cold PBS (2 ml) and treated with lysis buffer (500 µl) which consisted of 0.5% Nonidet P-40 and 0.5% sodium deoxycholate in PBS. The solution was transferred to safe-lock tubes for centrifugation at 6000g, 5 min, 4 °C. The supernatant was treated with 5 µl of proteinase K (1 µg/µl, Merck) for 30 min (37 °C), cooled on ice (2–3 min), followed by addition of phenylmethanesulfonyl fluoride (PMSF, 5 µl of 0.1 M solution) to stop the reaction. Then, 20 µl of glass fog solution 1% (Qbiogene Inc.) was added. The mixture was rolled over for 5 min and then centrifuged at 13,000g for 2 min. After removal of supernatant, the protein precipitate was dispersed in 20 µl of sample loading buffer and denatured for 5 min at 95 °C. On cooling to room temperature, the protein samples were loaded on to polyacrylamide SDS–PAGE gel for electrophoresis. Detection of PrP was done as described previously[29,30] using SAF83 (1:5000; SPI-Bio, France), a primary antibody against a human PrP fragment (amino acids 142–160), followed by an alkaline phosphatase-conjugated secondary antibody (anti-mouse IgG H&L, 1:20,000; Promega). Immunoreactive signals were visualized with CDP-Star detection reagent (Amersham) and were analyzed densitometrically with the ImageJ program (National Institute of Health, Bethesda, USA). Three independent assays were performed for each concentration of test compound.

6.3. Statistical analysis

EC_{50} and its 95% confidence intervals were obtained by nonlinear regression using the sigmoidal dose–response equation from GraphPad Prism 4.03.

Acknowledgments

This work was supported by National University of Singapore Academic Research Fund R148000064112 to GML and OWY, and Japanese Ministry of Health, Labor and Welfare Research Grant H19-nanji-006 to KD. Nguyen Thi Hanh Thuy gratefully acknowledged financial support (Research Scholarship) from Ministry of Education, Republic of Singapore and National University of Singapore for her graduate studies. We thank Fumi Toshioka and Keiko Nishizawa for technical assistances.

Supplementary data

Experimental procedures and analytical data for compounds **2–5**, **9**, **18**, **6**, **7**, **10–13**, **16**. Determination of purity of final compounds **5–8**, **10–20** by HPLC. Supplementary data associated with this article can be found, in the online version, at doi:10.1016/j.bmc.2008.05.060.

References and notes

1. Collinge, J. *Annu. Rev. Neurosci.* **2001**, *24*, 519.
2. Cashman, N. R.; Caughey, B. *Nat. Rev. Drug Disc.* **2004**, *3*, 874.
3. Caughey, B.; Caughey, W. S.; Kocisko, D. A.; Lee, K. S.; Silveira, J. R.; Morrey, J. D. *Acc. Chem. Res.* **2006**, *39*, 646.
4. Caughey, B.; Baron, G. S. *Nature* **2006**, *443*, 803.
5. Priola, S. A.; Raines, A.; Caughey, W. S. *Science* **2000**, *287*, 1503.
6. Webb, S.; Lekishvili, T.; Loeschner, C.; Sellarajah, S.; Prelli, F.; Wisniewski, T.; Gilbert, I. H.; Brown, D. R. *J. Virol.* **2007**, *81*, 10729.
7. Doh-ura, K.; Ishikawa, K.; Murakami-Kubo, I.; Sasaki, K.; Mohri, S.; Race, R.; Iwaki, T. *J. Virol.* **2004**, *78*, 4999.
8. Tracy, J. W.; Webster, L. T., Jr. In *Goodman and Gilman's The Pharmacological Basis of Therapeutics*; Hardman, J. G., Limbird, L. E., Eds.; McGraw Hill: New York, 2001; p 1111.
9. Doh-ura, K.; Iwaki, T.; Caughey, B. *J. Virol.* **2000**, *74*, 4894.
10. Korth, C.; May, B. C. H.; Cohen, F. E.; Prusiner, S. B. *Proc. Natl. Acad. Sci. U.S.A.* **2004**, *98*, 9836.
11. Barret, A.; Tagliavini, F.; Forloni, G.; Bate, C.; Salmona, M.; Colombo, L.; Luigi, A. D.; Limido, L.; Suardi, S.; Rossi, G.; Auvré, F.; Adjou, K. T.; Salès, N.; Williams, A.; Lasmézas, C.; Deslys, J. P. *J. Virol.* **2003**, *77*, 8462.
12. Collins, S. J.; Lewis, V.; Brazier, M.; Hill, A. F.; Fletcher, A.; Masters, C. L. *Ann. Neurol.* **2002**, *52*, 503.
13. Kobayashi, Y.; Hirata, K.; Tanaka, H.; Yamada, T. *Rinsho Shinkeigaku (Clin. Neurol.)* **2003**, *43*, 403.
14. Nakajima, M.; Yamada, T.; Kusuhara, T.; Furukawa, H.; Takahashi, M.; Yamauchi, A.; Kataoka, Y. *Dement. Geriatr. Cogn. Disord.* **2004**, *17*, 158.
15. May, B. C. H.; Fafarman, A. T.; Hong, S. B.; Rogers, M.; Deady, L. W.; Prusiner, S. B.; Cohen, F. E. *Proc. Natl. Acad. Sci. U.S.A.* **2003**, *100*, 3416.
16. Klingenstein, R.; Lober, S.; Kujala, P.; Godsave, S.; Leliveld, S. R.; Gmeiner, P.; Peters, P. J.; Korth, C. *J. Neurochem.* **2006**, *98*, 1696.
17. Dollinger, S.; Löber, S.; Klingenstein, R.; Korth, C.; Gmeiner, P. *J. Med. Chem.* **2006**, *49*, 6591.
18. May, B. C. H.; Witkop, J.; Sherrill, J.; Anderson, M. O.; Madrid, P. B.; Zorn, J. A.; Prusiner, S. B.; Cohen, F. E.; Guy, R. K. *Bioorg. Med. Chem. Lett.* **2006**, *16*, 4913.
19. Cope, H.; Mutter, R.; Heal, W.; Pascoe, C.; Brown, P.; Pratt, S.; Chen, B. *Eur. J. Med. Chem.* **2006**, *41*, 1124.
20. Figgitt, D.; Denny, W.; Chavalitshewinkoon, P.; Wilairat, P.; Ralph, R. *Antimicrob. Agents Chemother.* **1992**, *36*, 1644.
21. Chavalitshewinkoon, P.; Wilairat, P.; Gamage, S.; Denny, W.; Figgitt, D.; Ralph, R. *Antimicrob. Agents Chemother.* **1993**, *37*, 403.

22. Denny, W. A. *Curr. Med. Chem.* **2002**, *9*, 1655.
23. Goodell, J. R.; Svensson, B.; Ferguson, D. M. *J. Chem. Inf. Model.* **2006**, *46*, 876.
24. Breslow, D. S.; Walker, H. G.; Yost, R. S.; Shivers, J. C.; Hauser, C. R. *J. Am. Chem. Soc.* **1943**, *68*, 100.
25. Doh-ura, K.; Tamura, K.; Karube, Y.; Naito, M.; Tsuruo, T.; Kataoka, Y. *Cell. Mol. Neurobiol.* **2007**, *27*, 303.
26. Murakami-Kubo, I.; Doh-ura, K.; Ishikawa, K.; Kawatake, S.; Sasaki, K.; Kira, J.-i.; Ohta, S.; Iwaki, T. *J. Virol.* **2004**, *78*, 1281.
27. Klingenstein, R.; Melnyk, P.; Leliveld, S. R.; Ryckebusch, A.; Korth, C. *J. Med. Chem.* **2006**, *49*, 5300.
28. Ishikawa, K.; Kudo, Y.; Nishida, N.; Suemoto, T.; Sawada, T.; Iwaki, T.; Doh-ura, K. *J. Neurochem.* **2006**, *99*, 198.
29. Kawasaki, Y.; Kawagoe, K.; Chen, C. J.; Teruya, K.; Sakasegawa, Y.; Doh-ura, K. *J. Virol.* **2007**, *81*, 12889.
30. Doh-ura, K.; Kuge, T.; Umoto, M.; Nishizawa, K.; Kawasaki, Y.; Iha, M. *Antimicrob. Agents Chemother.* **2007**, *51*, 2274.

Journal of General Virology (2008), **89**, 1533–1544 DOI 10.1099/vir.0.83578-0

Effect of intraventricular infusion of anti-prion protein monoclonal antibodies on disease progression in prion-infected mice

Chang-Hyun Song,[1] Hidefumi Furuoka,[2] Chan-Lan Kim,[1]† Michiko Ogino,[1]‡ Akio Suzuki,[1] Rie Hasebe[1] and Motohiro Horiuchi[1]

Correspondence
Motohiro Horiuchi
horiuchi@vetmed.hokudai.ac.jp

[1]Laboratory of Prion Diseases, Graduate School of Veterinary Medicine, Hokkaido University, Kita 18, Nishi 9, Kita-ku, Sapporo 060-0818, Japan

[2]Department of Pathobiological Science, Obihiro University of Agriculture and Veterinary Medicine, Inada-cho, Obihiro 080-8555, Japan

It is well known that anti-prion protein (PrP) monoclonal antibodies (mAbs) inhibit abnormal isoform PrP (PrP^{Sc}) formation in cell culture. Additionally, passive immunization of anti-PrP mAbs protects the animals from prion infection via peripheral challenge when mAbs are administered simultaneously or soon after prion inoculation. Thus, anti-PrP mAbs are candidates for the treatment of prion diseases. However, the effects of mAbs on disease progression in the middle and late stages of the disease remain unclear. This study carried out intraventricular infusion of mAbs into prion-infected mice before and after clinical onset to assess their ability to delay disease progression. A 4-week infusion of anti-PrP mAbs initiated at 120 days post-inoculation (p.i.), which is just after clinical onset, reduced PrP^{Sc} levels to 70–80 % of those found in mice treated with a negative-control mAb. Spongiform changes, microglial activation and astrogliosis in the hippocampus and thalamus appeared milder in mice treated with anti-PrP mAbs than in those treated with a negative-control mAb. Treatment with anti-PrP mAb prolonged the survival of mice infected with Chandler or Obihiro strain when infusion was initiated at 60 days p.i., at which point PrP^{Sc} is detectable in the brain. In contrast, infusion initiated after clinical onset prolonged the survival time by about 8 % only in mice infected with the Chandler strain. Although the effects on survival varied for different prion strains, the anti-PrP mAb could partly prevent disease progression, even after clinical onset, suggesting immunotherapy as a candidate for treatment of prion diseases.

Received 9 November 2007
Accepted 28 February 2008

INTRODUCTION

Prion diseases, such as scrapie, bovine spongiform encephalopathy (BSE) and Creutzfeldt–Jakob disease (CJD), are fatal neurodegenerative disorders characterized by accumulation of a disease-specific, abnormal isoform of the prion protein (PrP^{Sc}) in the central nervous system (CNS), astrogliosis, neuronal vacuolation and neuronal cell death. The appearance of BSE and variant CJD (vCJD), possibly linked to consumption of food derived from BSE-infected cattle, has increased awareness of prion diseases, but at present there is no effective treatment available for prion diseases. Given that transformation of a normal prion protein (PrP^{C}) to PrP^{Sc} is a central event in the pathogenesis of prion disease, compounds and/or strategies that inhibit PrP^{Sc} formation are of therapeutic interest.

Many compounds or strategies have been reported to inhibit PrP^{Sc} formation, including polyanions, glycosaminoglycans, phosphorothioate oligonucleotides, tetrapyrroles, polyene antibiotics, tricyclic compounds, PrP peptides, dominant-negative PrP, cysteine protease inhibitors, PrP immunization and small interfering RNAs (reviewed by Trevitt & Collinge, 2006). Most of these compounds and treatments antagonize PrP^{Sc} formation in cells persistently infected with prions. However, the anti-prion effects *in vivo* are not always consistent with those observed *in vitro*. Indeed, some of the compounds and treatments protect animals from experimental inoculation with prions or delay the onset of disease when administered before, simultaneously or soon after inoculation with prions via a peripheral route (Ehlers & Diringer, 1984; Farquhar & Dickinson, 1986; Ladogana *et al.*, 1992; Priola

†Present address: Foreign Animal Disease Division, Animal Disease Control Department, National Veterinary Research and Quarantine Service, 480 Anyang-6 dong, Manan-gu, Anyang 430-824, Republic of Korea.

‡Present address: Institute of Tropical Medicine, Nagasaki University, 1-12-4 Sakamoto, Nagasaki 852-8523, Japan.

et al., 2000). In addition, only a few compounds, such as amphotericin B, its derivative, MS-8209 and pentosan polysulfate (PPS), can prolong survival of mice infected with prions even when administered in the middle or late stage of prion infection via intracerebral inoculation (Demaimay *et al.*, 1997; Doh-ura *et al.*, 2004). Because intraventricular infusion of PPS at a late stage prolongs the incubation period of the disease in transgenic mice that overexpress PrP (Doh-ura *et al.*, 2004), clinical trials using PPS to treat human prion diseases are moving forward (Todd *et al.*, 2005). The current evidence suggests that PPS treatment of vCJD patients appears to have some beneficial effects, although the specificity of the effects still needs to be evaluated carefully (Rainov *et al.*, 2007).

Anti-PrP antibodies prevent direct interaction between PrP^{C} and PrP^{Sc} in a cell-free conversion reaction (Kaneko *et al.*, 1995; Horiuchi & Caughey, 1999). Subsequent reports have shown that anti-PrP antibodies prevent prion propagation in cells persistently infected with prion (Enari *et al.*, 2001; Peretz *et al.*, 2001; Gilch *et al.*, 2003; Kim *et al.*, 2004b; Perrier *et al.*, 2004; Feraudet *et al.*, 2005). The inhibitory effect of anti-PrP antibodies has also been demonstrated *in vivo*. Transgenic mice expressing monoclonal antibody (mAb) 6H4 were shown to be resistant to prion infection via the intraperitoneal route (Heppner *et al.*, 2001). Moreover, active immunization with recombinant PrP, synthetic PrP peptide or a DNA vaccine has been shown to delay the onset of the disease in mice following peripheral prion infection, although immunization was a prerequisite to obtain the prophylactic effect (Sigurdsson *et al.*, 2002; Schwarz *et al.*, 2003; Goñi *et al.*, 2005; Fernandez-Borges *et al.*, 2006). Passive immunization with anti-PrP antibodies was found to be effective in preventing prion infection via the peripheral route if antibodies were administered shortly after prion inoculation, but was not following intracerebral prion infection or if administered on or after clinical onset following intraperitoneal prion infection (White *et al.*, 2003). These results suggest that anti-PrP antibodies can protect against establishment of prion infection in peripheral tissues and thus may be useful for post-exposure prophylaxis. However, the therapeutic potential of anti-PrP antibodies, including whether or not anti-PrP antibodies antagonize prion propagation in the brain and can inhibit disease progression when applied after clinical onset, remains to be elucidated.

To evaluate the therapeutic effects of anti-PrP antibodies on prion diseases more precisely, we carried out intraventricular infusion of anti-PrP mAbs in mice that had been inoculated intracerebrally with prions. Here, we show that intraventricular infusion of anti-PrP mAbs reduced the level of accumulation of PrP^{Sc} and reduced spongiform changes and gliosis relative to negative controls. Furthermore, we observed prolongation of the incubation time in mice infected with the Chandler strain, even when infusion was initiated at the time of clinical onset of the disease.

METHODS

Antibodies. The following anti-PrP mAbs were used in this study: 106 (IgG2b), 110 (IgG2b), 31C6 (IgG1) and 44B1 (IgG2a). The mAbs 106, 110 and 31C6 recognized linear epitopes consisting of mouse PrP aa 88–90, 83–89 and 143–149, respectively, whereas mAb 44B1 recognized a discontinuous epitope within aa 155–231 (Kim *et al.*, 2004a). Anti-feline parvovirus mAb P2-284 (IgG1) was used as a negative control (Horiuchi *et al.*, 1997). The mAbs were dialysed for 3 days against PBS prior to intraventricular infusion. An Alexa Fluor 488 Protein Labelling kit (Molecular Probes) was used for fluorescent labelling of mAbs.

The following rabbit polyclonal antibodies were used as primary antibodies for immunohistochemistry: B103, which recognizes bovine PrP synthetic peptide aa 103–121 (Horiuchi *et al.*, 1995), anti-glial fibrillary acidic protein (GFAP; Dako) to visualize astrocytes and anti-Iba1 (Wako) to visualize microglia.

Mice and prion strains. All procedures for animal experiments were carried out according to protocols approved by the Institutional Committee for Animal Experiments. Mouse-adapted scrapie strains Obihiro and Chandler were used in this study. For intracerebral inoculation, 4-week-old female ICR mice were purchased from CLEA Japan. Twenty microlitres of 10 % brain homogenate from mice infected with the Obihiro or Chandler strain was injected into the left hemisphere. Twelve-week-old female ICR mice were used to determine the distribution of mAbs and to analyse neuronal toxicity by anti-PrP mAbs.

Intraventricular infusion of mAbs using an osmotic pump. Alzet Mini-Osmotic Pumps, models 2001, 2002 and 2004 (DURECT), were used in this study. Filling of the osmotic pumps with antibody solution was carried out according to the manufacturer's instructions. The pre-filled pumps were then placed in PBS at 37 °C for 24 h. Mice were fitted with a stainless steel cannula supplied with the Alzet Brain Infusion kit (DURECT) and positioned according to stereotaxic coordinates into the left lateral ventricle of the brain (bregma – caudal 1.0 mm, lateral 1.0 mm with a depth of 3 mm below the dura). The osmotic pumps were subsequently implanted subcutaneously into the back and connected to the fitted cannula. All surgical procedures were performed under anaesthesia by intramuscular injection of xylazine (10 mg kg^{-1}) and ketamine (50 mg kg^{-1}). After surgery, cefotaxime (Chugai) was administered subcutaneously (40 mg kg^{-1}) and a gentamicin ointment (Schering-Plough) was pasted on the suture line for 3 days. All mice were housed individually during post-surgery observation periods. Mice that died within a few days of the operation were excluded from the statistical analysis.

Stereotaxic injection of mAbs. Mice were anaesthetized as described above and placed onto a stereotaxic apparatus (Narishige). A linear scalp incision was made and the skull was exposed. Bilateral burr holes were drilled to accommodate stereotaxic placement into the left and right hippocampus (bregma – caudal 2.0 mm, lateral 2.1 mm). Using a Hamilton syringe with a 31-gauge needle, 2 µl mAbs (2 mg ml^{-1}) were injected into the left and right hippocampus, respectively, at a depth of 2 mm below the dura. Injection was carried out over a period of 15 min.

Western blotting. Brains were sagittally hemi-sectioned and homogenized in 10 % (w/v) TMS buffer [50 mM Tris/HCl (pH 7.5), 5 mM $MgCl_2$, 5 % glucose]. To detect PrP^{Sc}, 200 µl brain homogenate was mixed with an equal volume of a detergent buffer [8 % Zwittergent 3-14, 1 % Sarkosyl, 100 mM NaCl, 50 mM Tris/HCl (pH 7.5)] and treated with collagenase (0.5 mg ml^{-1}) for 15 min at 37 °C. The samples were then digested with proteinase K (PK; Roche)

at 20 μg ml^{-1} for 30 min at 37 °C. After terminating PK activity by adding Pefabloc (Roche) at 2 mM, samples were treated with 40 μg DNase I ml^{-1} for 5 min. A half volume of a mixture of 2-butanol and methanol (5:1) was added and the PrP^{Sc} was pelleted by centrifugation at 20 000 **g** for 10 min at 20 °C. The resulting pellet was dissolved in 1 × SDS sample buffer [62.5 mM Tris/HCl (pH 6.8), 5 % glycerol, 3 mM EDTA, 4 % β-mercapthoethanol, 0.04 % bromophenol blue, 5 % SDS, 4 M urea] by boiling for 5 min. SDS-PAGE and Western blotting were carried out as described elsewhere (Uryu *et al.*, 2007)

Histopathology and immunohistochemistry. Mouse brains that had been infused with Alexa Fluor 488-conjugated mAbs were frozen in Tissue-Tek OCT compound (Sakura) and cryosections of 16–20 μm were prepared. The sections were dried and fixed with acetone for 10 min. Sections were mounted with Vectashield containing propidium iodine (PI; Vector Laboratories) and examined with a Nikon C1 laser confocal microscope. The presence of infused mAb was also confirmed by direct detection as follows. The sections were reacted with EnVision$^+$ System-labelled polymer conjugated to horseradish peroxidase (HRP) (Dako) for 45 min at 37 °C and positive signals were detected using Simple Stain 3,3′-diaminobenzidine (DAB) solution (Nichirei). This was followed by counterstaining with Mayer's haematoxylin (Wako).

Dissected mouse brains were fixed in 10 % formalin and embedded in paraffin. Sections (4 μm) were deparaffinized, rehydrated and subjected to haematoxylin and eosin (H&E) staining or immunohistochemistry. Antigen retrieval for immunohistochemistry was performed by hydrolytic autoclaving at 135 °C for 20 min for detection of PrP^{Sc} and at 121 °C for 10 min for GFAP and Iba1 (Furuoka *et al.*, 2005). The sections were treated with 3 % H_2O_2 for 5 min, blocked with 10 % normal goat serum for 30 min and then incubated for 45 min at 37 °C with B103 at a dilution of 1 : 100, anti-GFAP at 1 : 5000 or anti-Iba1 at 1 : 100. After washing with PBS, the sections were reacted with EnVision$^+$ System-labelled polymer–HRP for 45 min at 37 °C. The sections were then rinsed and developed with Simple Stain DAB, followed by counterstaining with Mayer's haematoxylin.

Terminal uridine deoxynucleotidyl transferase dUTP nick end labeling (TUNEL) staining. Neuronal cell death was examined using an *In situ* Cell Death Detection kit (Roche). Four micrometer sections of paraffin-embedded brain tissue were deparaffinized, rehydrated and incubated with 10 μg PK ml^{-1} for 10 min at 37 °C. After washing with PBS, the sections were incubated with labelling mixture containing terminal deoxynucleotidyl transferase and digoxigenin-labelled dUTP-conjugated FITC for 60 min at 37 °C. The sections were counterstained with PI and examined with a C1 laser confocal microscope.

RESULTS

Distribution of mAb in brain following intraventricular infusion

We first examined the distribution of mAb infused into the left lateral ventricle of mouse brain. Alexa Fluor 488-conjugated mAb 31C6 (anti-PrP mAb) or P2-284 (negative-control mAb) was infused into the left lateral ventricle and the distribution of mAb was examined at 7, 14, 24 and 34 days after the initiation of infusion. To examine the distribution of the mAbs, brain cryosections at the levels indicated in Fig. 1(a) were prepared. Fig. 1(c) shows the detection of Alexa Fluor 488-conjugated mAb 31C6 in the hippocampus. Fluorescence was detected over the hippocampus (up to 14 days). Although the area of distribution gradually narrowed thereafter, mAbs were still detectable in the hippocampus at 20 days after the termination of infusion (i.e. at 34 days). In contrast, a very low-level fluorescent signal was detected in the hippocampus of a mouse infused with Alexa Fluor 488-conjugated mAb P2-284, even at 7 days after the initiation of infusion. These results suggested that the longer duration of mAb 31C6 in the hippocampus compared with the control mAb was due to binding of mAb 31C6 to PrP^{C}.

Fig. 1(d) summarizes the distribution of the anti-PrP mAb. The mAb was well distributed to areas surrounding the lateral and dorsal third ventricles, hippocampus and thalamus. The mAb was also detected in areas close to the ventral third ventricles. In addition, mAb was detected in regions of the medulla oblongata that face the fourth ventricle and the subarachnoid space, suggesting that the mAb infused into the lateral ventricle was distributed to many parts of brain, presumably via the flow of cerebrospinal fluid. Although the mAb was distributed to parts of the brain parenchyma, distribution of mAb into the cortex and cerebellum appeared to be less efficient. When observing sections under a microscope, we noticed that the mAb-infused hemisphere showed higher fluorescence intensity than that observed in the contralateral side (data not shown), suggesting that the distribution of mAb was not symmetrical. This tendency was confirmed by direct detection of Alexa Fluor 488-conjugated mAb 31C6 (Fig. 1b).

Effects of anti-PrP mAbs on PrP^{Sc} accumulation in the brain

Mice inoculated with Obihiro or Chandler strain reach the terminal stage of the disease at around 150 days post-inoculation (p.i.). Early clinical signs such as ataxia of hind limbs and changes in pelage and posture appear at around 120 days p.i. To evaluate the therapeutic potential of anti-PrP mAbs in a late stage of the disease, infusion of mAbs was started at 120 days p.i. and accumulation of PrP^{Sc} and neurohistopathological lesions were analysed.

Fig. 2(a) shows PrP^{Sc} accumulation in the brains of mice infected with the Obihiro strain at 30 days post-infusion (150 days p.i.). The mean PrP^{Sc} levels in mice treated with mAbs 110, 31C6 and 44B1 were 78, 69 and 77 %, respectively, compared with the control (mAb P2-284; n=2). To determine whether the relative reduction in PrP^{Sc} levels was caused by acceleration of PrP^{Sc} degradation or deceleration of PrP^{Sc} accumulation, we analysed the kinetics of PrP^{Sc} accumulation during the period from 127 to 150 days p.i. (Fig. 2b). There was no difference in PrP^{Sc} levels in mice treated with anti-PrP mAbs compared with those treated with the negative-control mAb at 127 days p.i. (7 days after the initiation of infusion). However, PrP^{Sc} levels increased 2.3-fold in mice treated with the control

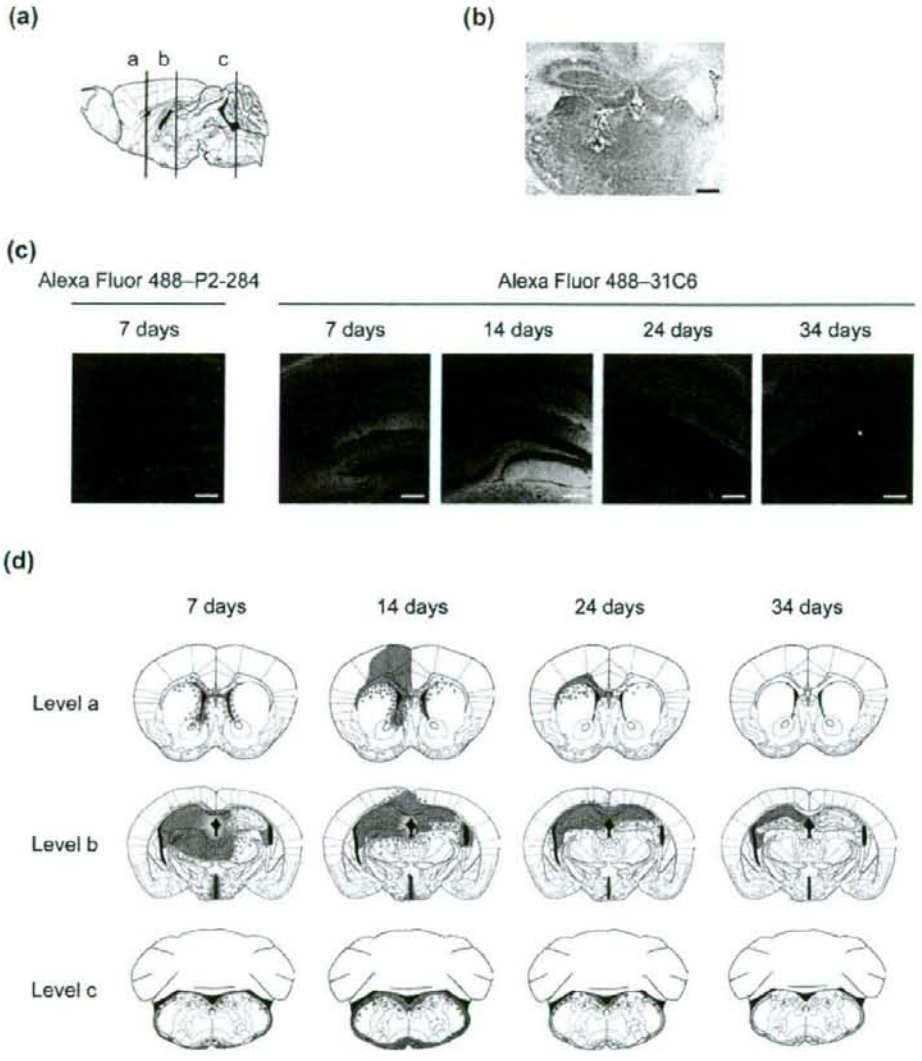

Fig. 1. Distribution of mAbs following intraventricular infusion. Alexa Fluor 488-conjugated mAb 31C6 or P2-284 was infused into the left lateral ventricle using an Alzet Mini-Osmotic Pump model 2002 (mAb concentration 0.5 mg ml^{-1}, pumping rate 0.5 µl h^{-1}, duration 14 days, volume 200 µl). (a) Levels of coronal section examined. Cryosections at the indicated levels were prepared. (b) Detection of mAbs by direct staining. A frozen section at level b was prepared from the brain of a mouse sacrificed at 5 days after starting infusion and the distribution of mAb was visualized by direct staining. Bar, 500 µm. (c) Detection of mAbs in the hippocampus. mAbs conjugated with Alexa Fluor 488 were analysed by laser confocal microscopy. Bars, 200 µm. (d) Distribution of mAb after infusion. The distribution of mAb at 7, 14, 24 and 34 days after starting infusion (green) was superimposed on the images taken from Paxinos & Franklin (2001).

mAb over the period 127–150 days p.i., whereas PrP^{Sc} levels increased only 1.6-, 1.3- and 1.3-fold in mice treated with mAbs 110, 31C6 and 44B1, respectively. These results indicated that anti-PrP mAbs can reduce the rate of PrP^{Sc} accumulation in the brain, even when treatment is initiated at a late stage of the disease.

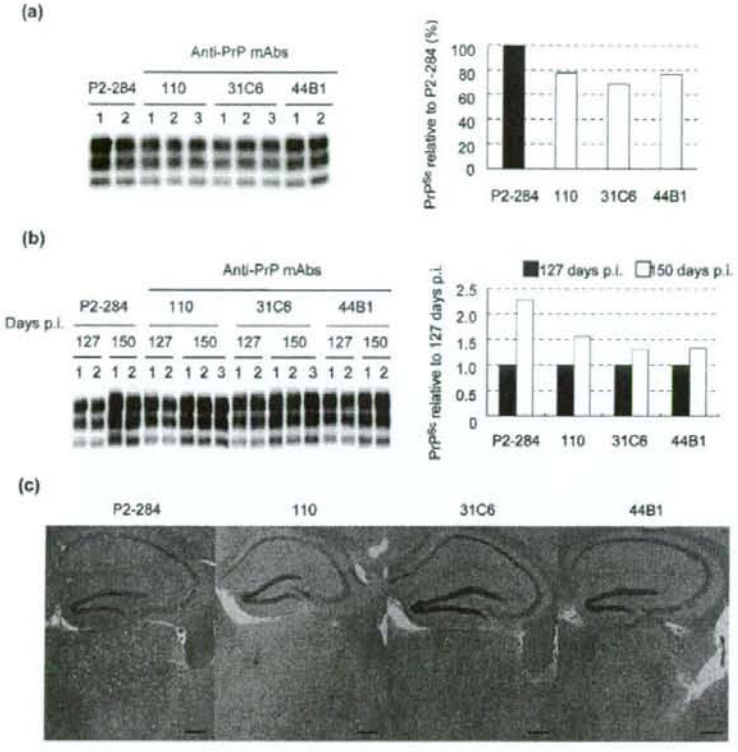

Fig. 2. Effects of anti-PrP mAbs on PrP^{Sc} accumulation and spongiform changes in mice infected with the Obihiro strain. mAbs were infused into the left lateral ventricle of mice inoculated with the Obihiro strain at 120 days p.i. using an Alzet Mini-Osmotic Pump model 2004 (mAb concentration 2 mg ml^{-1}, pumping rate 0.25 µl h^{-1}, duration 28 days, volume 200 µl). Mouse brains were cut sagittally along the midline. The left hemisphere (mAb-infused side) was used for the detection of PrP^{Sc} by Western blotting, whereas the right hemisphere (non-infused side) was fixed with 10 % formalin for paraffin sections. (a) Accumulation of PrP^{Sc} at 150 days p.i. Samples from individual mice (50 µg brain equivalent) were loaded in each lane and the intensities of PrP^{Sc} bands were quantified. The mean intensity for mice treated with the negative-control mAb (P2-284) was designated 100 % and the graph shows relative PrP^{Sc} levels for mice treated with anti-PrP mAbs. (b) Kinetics of PrP^{Sc} accumulation. Mice were sacrificed at 127 and 150 days p.i. and the left hemisphere (mAb-infused side) was used for Western blotting. Samples from individual mice (50 µg brain equivalent) were loaded in each lane and chemiluminescence intensities were quantified. The graph on the right shows the mean level of PrP^{Sc} at 150 days p.i. compared with the level at 127 days p.i. Samples at 150 days p.i. were the same as those in (a). (c) Spongiform changes at 150 days p.i. Paraffin sections were prepared from the contralateral hemisphere of the brain described in (a) and stained with H&E.

Effects of anti-PrP mAbs on neurodegeneration

Next, we investigated the effects of mAbs on neurodegeneration. To do this, the contralateral hemispheres of brains used in Fig. 2(a) (at 150 days p.i.) were examined histopathologically. Although mAbs were more readily detected in the infused side than in the contralateral side (Fig. 1), spongiform changes in the hippocampus and thalamus of mice treated with mAbs 110, 31C6 and 44B1 were nevertheless milder than those treated with the negative-control mAb (Fig. 2c).

Immunohistochemical examination also revealed that anti-PrP mAbs affected the progression of neuropathological lesions in mice infected with the Obihiro strain (Fig. 3). Consistent with the reduction in PrP^{Sc} levels by anti-PrP mAbs (Fig. 2a), PrP^{Sc} deposition in the hippocampus and thalamus of mice infused with mAbs 110 and 31C6 was milder than in the negative control. In addition, astrogliosis (as evaluated by GFAP staining) appeared to be reduced in mice treated with anti-PrP mAbs compared with the negative control. Microglial activation in the

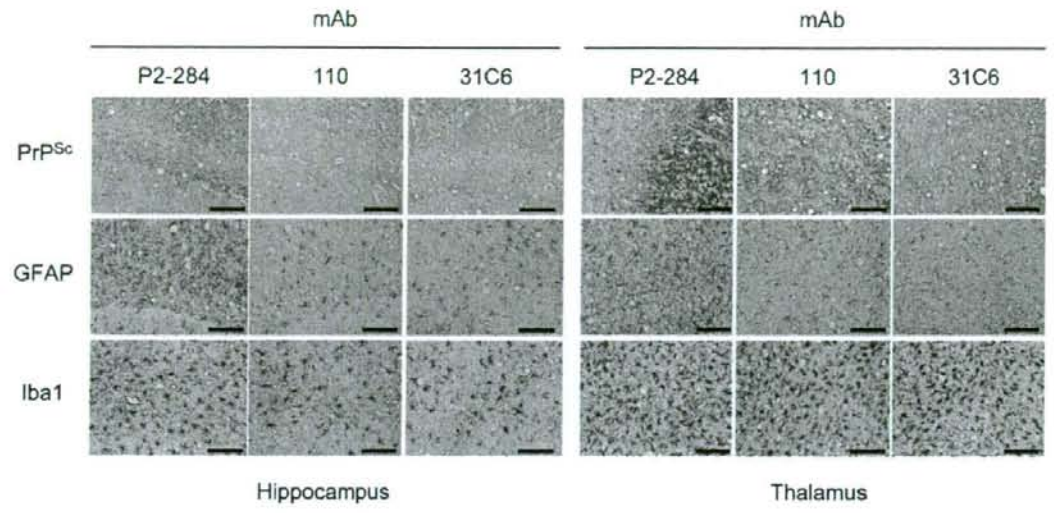

Fig. 3. Effects of anti-PrP mAbs on PrP^{Sc} accumulation and gliosis in mice infected with the Obihiro strain. Intraventricular infusion of mAbs was carried out as described in Fig. 2 and brains collected at 150 days p.i. were used for analysis. The mice shown in this figure belonged to an independent experimental group (i.e. different from the experimental group shown in Fig. 2). Paraffin-embedded sections were stained with B103 antibodies to detect PrP^{Sc}, anti-GFAP antibodies to detect astrocytes and anti-Iba1 antibodies to detect microglia. Images of the hippocampus and thalamus are indicated. All images represent the mAb-infused side. Bars, 200 μm.

hippocampus (as detected with anti-Iba1 antibodies) was also reduced in the presence of anti-PrP mAbs; in contrast, the effect was marginal in the thalamus.

To investigate the effects of anti-PrP mAbs on different prion strains, we carried out the same experiment using mice infected with the Chandler strain. Similar to what was observed for mice infected with the Obihiro strain, in mice infected with the Chandler strain, mAb 31C6 reduced spongiform changes and PrP^{Sc} deposition in the hippocampus and thalamus compared with the negative-control mAb (Fig. 4). However, the effect of anti-PrP mAb on gliosis appeared to differ for the two different prion strains. Anti-PrP mAbs apparently reduced astrogliosis in the hippocampus and thalamus of mice infected with the Obihiro strain (Fig. 3), but only a slight reduction in astrogliosis was observed for mice infected with the Chandler strain (Fig. 4). Moreover, although microglial activation in the thalamus of mice infected with the Obihiro strain was slightly reduced by treatment with anti-PrP mAbs, it was obviously reduced relative to controls by treatment with mAb 31C6 in mice infected with the Chandler strain (Fig. 4). However, microglial activation as a whole appeared to be moderate in mice infected with the Chandler strain compared with the Obihiro strain; thus, the difference observed could be due to a difference in the level of activation of the microglia between mice infected with the two prion strains.

Prolongation of survival time

To determine whether treatment with anti-PrP mAbs can prolong survival of prion-infected mice when administered at different stages in progression of the disease, infusion was started at a middle stage of infection (60 or 90 days p.i.) and after clinical onset (120 days p.i.). In mice infected with the Obihiro strain, infusion of mAb 31C6 initiated at 60 days p.i. prolonged survival by about 11 days compared with the negative control; however, no effect was observed when infusions were initiated at 90 or 120 days p.i. (Fig. 5 and Table 1). In contrast, for mice infected with the Chandler strain, prolongation of survival was observed in all three groups: infusion initiated at 60, 90 or 120 days p.i. prolonged survival by approximately 10, 13 or 12 days, respectively. Brain sections (H&E stained) of all mice were examined for possible causes of death other than prion disease. Of 96 mice tested, two had severe abscesses around the infused area and thus were excluded from the experimental group.

Changes in body weight were consistent with prolonged survival times. For experimental groups in which survival was prolonged by infusion with mAb 31C6, the decrease in body weight observed in control groups was delayed by about 1 or 2 weeks (Fig. 6). In contrast, no difference was observed for mice infected with the Obihiro strain when mAb infusion was started at 90 or 120 days p.i.

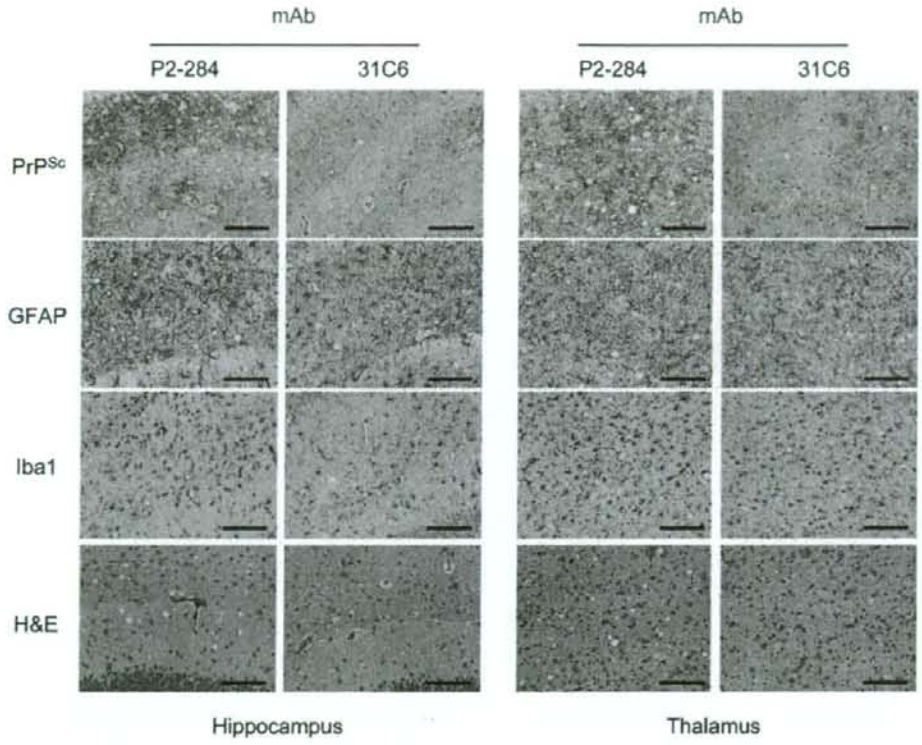

Fig. 4. Effects of anti-PrP mAbs on neuropathological changes in mice infected with the Chandler strain. Intraventricular infusion of mAbs was carried out as described in Fig. 2 using mice inoculated with the Chandler strain and brains collected at 150 days p.i. were used for analysis. The hippocampus and thalamus from mAb-infused hemispheres are shown. Bars, 100 μm.

Neuronal toxicity of mAbs

As it has been reported that an anti-PrP mAb recognizing aa 95–105 of murine PrP can induce apoptosis in hippocampal neurons (Solforosi *et al.*, 2004), we assessed the neurotoxicity of the mAbs used in this study. First, mAbs were infused into the lateral ventricle for 7 days using an Alzet Mini-Osmotic Pump model 2001 (mAb concentration 1 mg ml^{-1}, pumping rate 1 μl h^{-1}, duration 7 days, volume 200 μl); however, no difference was observed between mice treated with anti-PrP mAbs and those treated with the negative-control mAb (data not shown). To assess neurotoxicity directly, we next stereotaxically injected anti-PrP mAbs and the control mAb into the left and right hippocampus, respectively. The distribution of mAb in the hippocampus was confirmed by injecting Alexa Fluor 488-conjugated mAb 31C6 (Fig. 7a). Although mAb was well-distributed throughout the entire hippocampus on the injected side, TUNEL-positive cells were only detected in a limited area of the pyramidal layer and this was observed even in the right side (the side injected with the control mAb P2-284). Indeed, the TUNEL-positive cells were close to the injection site, suggesting that the TUNEL-positive cells resulted from the trauma of mAb injection. It was interesting that mAbs 106 and 110 recognizing the region adjacent to aa 95–105 did not induce apparent neuronal death.

DISCUSSION

In this study, we investigated the effects of anti-PrP mAbs on progression of prion disease, focusing on treatment during late stages of infection. We showed that anti-PrP mAbs antagonized PrP^{Sc} formation in the brain when intraventricular administration was initiated at the time of clinical onset (Figs 2 and 3). The effect of anti-PrP mAbs appeared to be mainly due to deceleration of PrP^{Sc} formation rather than active degradation of PrP^{Sc}. Several reports have suggested that binding of anti-PrP antibodies to the first α-helical domain of PrP^{C} (aa 143–155), which is proposed to be important for the PrP^{C}–PrP^{Sc} interaction (Morrissey & Shakhnovich, 1999; Speare *et al.*, 2003), prevents PrP^{Sc} formation by inhibiting the direct inter-